

Functional MRI

Peter A. Bandettini *

Unit on Functional Imaging Methods, Laboratory of Brain and Cognition, National Institute of Mental Health, Building 10, Room 1D80, 10 Center Drive MSC 1148, Bethesda, MD 20892-1148, USA

Introduction

Functional MRI (fMRI) has been in existence for about eleven years (Bandettini, Wong, Hinks et al., 1992; Blamire, Ogawa, Ugurbil et al., 1992; Frahm, Bruhn, Merboldt et al., 1992; Kwong, Belliveau, Chesler et al., 1992; Ogawa, Tank, Menon et al., 1992). During this time, the technique has experienced explosive growth. The reasons for this growth include the following: (a) demonstrated robustness and reproducibility; (b) minimal invasiveness; (c) the wide availability of the necessary hardware; (d) the unique functional spatial and temporal resolution niche that it fills; (e) the increasing accuracy of the interpretation of the functional contrast; and, importantly, (f) the potential that it promises.

The evolution of fMRI as a whole can perhaps be better understood as the co-development of four components. Each component can open up new advancement possibilities for the others, and likewise, a need in one component can focus or motivate the development of the other components. These four co-evolving components create the structure of this chapter. They are: Technology, methodology, interpretation, and applications. The history of fMRI can be sketched from this four-component perspective. Fig. 1 is an attempt to graphically illustrate a time line of the advancement of many, but certainly not all, significant aspects of each component. The times

are approximate and of course many categories are left out. This is simply an attempt to illustrate how each component has evolved in parallel.

The technology component consists of the hardware, pulse sequences used, and devices used for subject interface and handling. The methodology component primarily consists of mannerisms by which the fMRI experiment is carried out, intimately related to the subsequent processing methods. The interpretation component consists of all the advancements that have taken place towards better understanding the fMRI signal change dynamics, magnitude, linearity, and heterogeneity. Lastly, the application component is typically the receiver of these advancements but is also the driver of the development of the other three components. In this chapter, each component is described, with greater emphasis placed on the technology, methodology, and interpretation components of fMRI.

Technology

It is tool advancement that has driven and continues to drive the development of fMRI more than anything. Without the ability to perform high-speed imaging, in particular echo-planar imaging (EPI), and without the creation of magnets of 1.5 Tesla or higher, functional MRI would not at all be where it is now. This section overviews the major technological advances and issues related to fMRI, including the advancements of field strength, gradient, and pulse sequence technology. Pulse sequences are described from the perspective of the achievement of high

* Tel.: +1-301-402-1333; Fax: +1-301-402-1370;
E-mail: bandettini@nih.gov

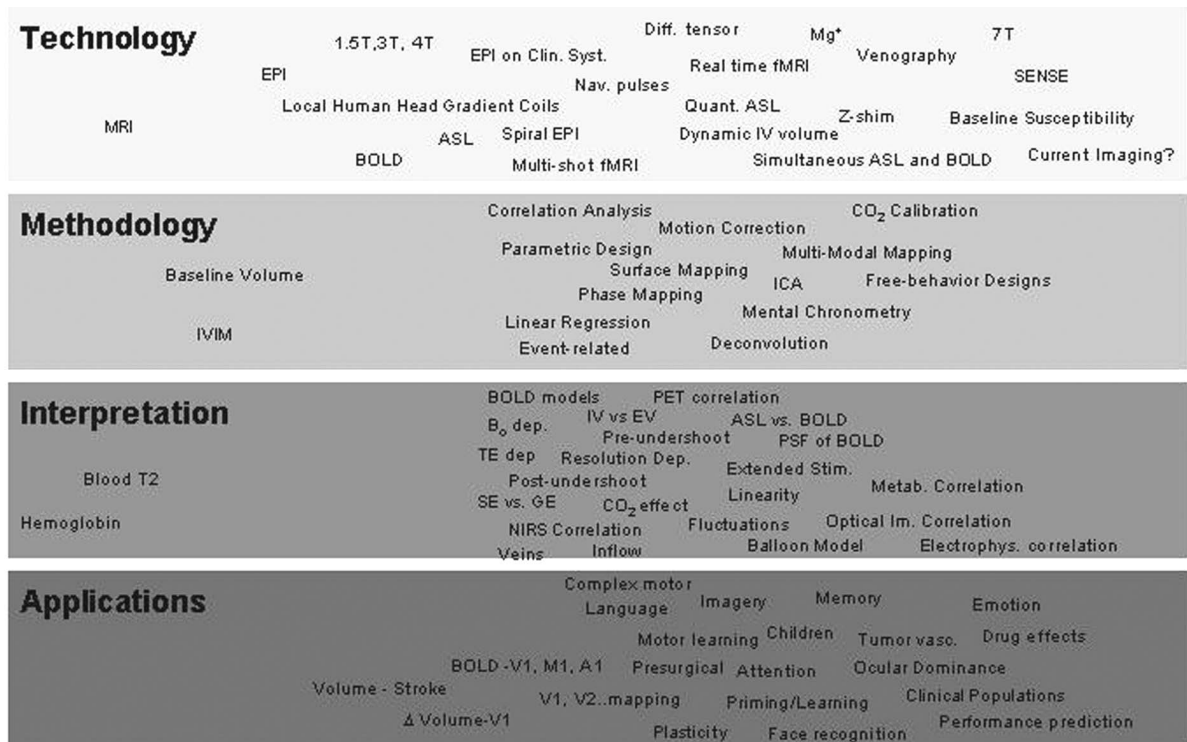


Fig. 1. Approximate timetable delineating some, but of course, not all major developments related to functional MRI within the categories of technology, methodology, interpretation, and applications.

temporal and spatial resolution as well as that of obtaining of more specific functional information. I strongly feel that it is important for all fMRI practitioners to at least have some perspective of the issues involved with pushing the technology. All of the text is specifically written to be readable by a non-specialist.

Hardware

As a guide, a drawing of the basic components of an MRI scanner is shown in Fig. 2. Protons precess at a frequency that is proportional to the magnetic field that they are experiencing. At higher frequencies, the magnetic moment of protons, and therefore the amount of signal produced, is greater. This relationship is linear. Functional MRI contrast also increases

approximately linearly with field strength (Gati, Menon, Ugurbil and Rutt, 1997; Menon, Ogawa, Tank and Ugurbil, 1993; Turner, Jezzard, Wen et al., 1993). In addition, at higher field strengths, blood oxygenation level-dependent (BOLD) contrast is thought to be more specific to capillaries (Gati et al., 1997; Lee, Silva, Ugurbil and Kim, 1999). This increased signal-to-noise, functional contrast, and specificity has driven the creation of higher field strength magnets for human functional MRI. In 1984, 1.0 T was considered high. In 1988, 1.5 T was considered high. In 1993, 3 and 4 T were at the upper end of what was considered high. In 1998, the FDA approved the first 3-T magnets for clinical use, accelerating mass production of such magnets. At this point in time, 7 T to 8 T are considered ‘high’ fields for human imaging. The progression continues. Hu-

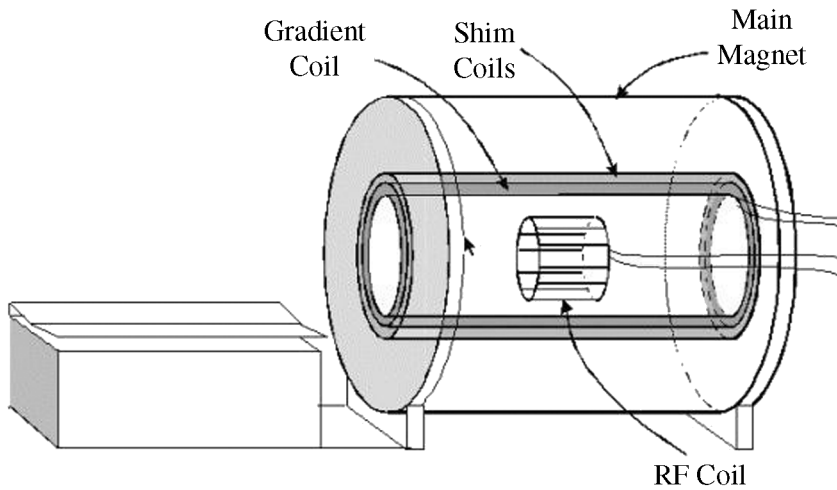


Fig. 2. Basic diagram of the MRI scanner. The primary coils are the superconducting coil to create the main magnetic field, the shim coils, the gradient coil, and the RF excitation and receive coils.

TABLE 1
Advantages and disadvantages of high field strength functional MRI

Advantages	Disadvantages
Signal to noise is linearly proportional to field strength.	In fMRI, what matters is temporal signal to noise, which does not scale with field strength at typical (low) resolutions since physiologic fluctuations, independent of field strength, contribute significantly. This will blunt the B_0 -based gains in S/N and functional contrast to noise.
Functional contrast to noise increases with B_0 , allowing comparisons of subtler signal changes or allowing for shorter scans for similar quality functional maps.	Baseline T_2^* and T_2 also decrease with B_0 , therefore lowering the TE at which optimal contrast is obtained, reducing the gain in functional contrast to noise somewhat.
High signal to noise allows higher resolution to be obtained.	To achieve the high resolution, one needs a longer readout window (difficult at higher field strengths) or multi-shot imaging (time consuming and more temporally unstable).
Blood T_1 increases, increasing functional contrast for arterial spin labeling (ASL) perfusion imaging techniques. It is thought that at just above 7 T, perfusion and BOLD functional contrasts are similar.	At typical fMRI resolutions, signal dropout is greater at higher field strengths, requiring better shimming techniques and/or smaller voxel sizes.
At field strengths of 3 T or above, vein T_2^* becomes much less than gray matter T_2^* , making the creation of venograms a simple matter of collecting a high-resolution T_2^* scan.	RF power deposition issues are more significant at higher field strengths, therefore limiting continuous arterial spin labeling techniques and high-resolution fast spin-echo imaging.
At field strengths of 9 T or greater, intravascular contribution is gone, therefore enabling more precise functional localization.	It is more difficult to create a homogeneous RF power deposition at higher field strengths.

man scanners in the range of 9–12 T are being designed and built. Higher fields of course cost more to create and are accompanied with their own technical hurdles. The advantages and disadvantages of high field strength are outlined in more detail in Table 1.

Because of high functional contrast and high signal to noise, higher fields are considered more advantageous than lower fields for functional MRI. To realize these advantages, many difficulties need to be overcome. For ‘standard’ fMRI applications,

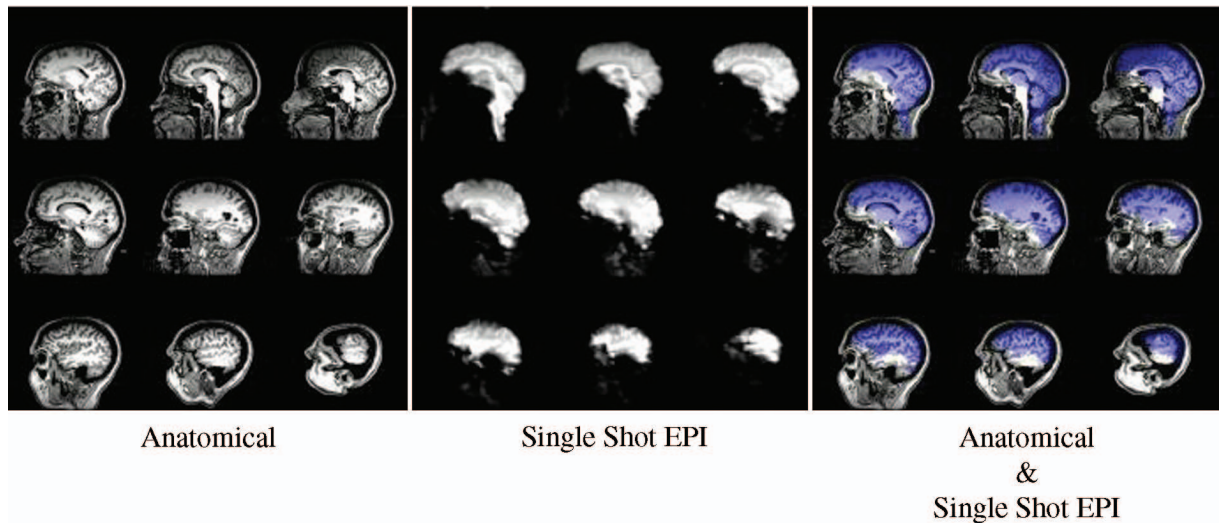


Fig. 3. Depiction of the signal dropout and warping characteristic of echo-planar imaging (EPI) at 3 T. Signal dropout is influenced by relative field inhomogeneity. The effects of this can be modulated by voxel size and dimension. Image warping is influenced by field inhomogeneity and readout window duration. The shorter the window duration, the less the warping effects. The image set on the left is a typical high-resolution, multi-shot anatomical scan. The image set in the middle consists of the same anatomical locations but obtained using EPI (64×64 matrix size). Voxel dimension ($3.12 \times 3.12 \times 5$ mm). The image on the right shows the echo-planar images superimposed, in blue, over the anatomical scans. (Image courtesy of E. Kapler and P. Bellgowan.)

1.5 T is considered the threshold minimum field strength. For imaging at the base of the brain or near sinuses or air passages, it may very well be the only field currently able to successfully do it while also allowing whole-brain imaging at the same time (without advanced shimming methods). Methods to combat signal dropout at higher field strengths include: shortening the echo time (TE), reducing the voxel volume (or at least the voxel dimension perpendicular to the susceptibility gradient), performing localized shimming, or performing techniques such as z-shim. A sobering example of the somewhat dramatic difference in image quality and coverage between typical EPI collection and standard anatomical imaging at 3 T is shown in Fig. 3. The EPI set is overlaid in blue on the anatomical set. The areas that are not blue are completely missed by EPI.

For extremely high-resolution functional imaging (i.e. sub-millimeter voxel volumes), multi-shot EPI (to achieve the necessary spatial resolution) and field strengths at or above 4 T or above (to provide a high enough signal-to-noise ratio) are required (Cheng, Waggoner and Tanaka, 2001; Menon and Goodyear, 1999; Menon, Ogawa, Strupp and Ugurbil, 1997). Functional MRI at 3 T may be the best

compromise between sensitivity and signal dropout when performing whole-brain imaging. A key piece of developing technology, along with RF coil technology, that will allow for whole-brain imaging at higher field strength is that involving shimming or pulse-sequence-based correction of magnetic field distortion effects, such as z-shimming (i.e. Glover, 1999a). This technology has very much room for improvement.

These improvements in shimming can be realized by increasing the electric current and voltage to shim coils, increasing the number of shim coils and their proximity to the brain, and perhaps working with non-orthogonal shim coil strategies. Lastly, if the current or voltage to shim coils is increased, then a separate shim setting for each slice may be used and switched between each image acquisition, allowing a much more robust and specific method for magnetic field inhomogeneity compensation. These are all advancements for the future.

Magnetic field gradient creation and modulation is a necessary step to spatially encode protons and therefore create an MR image. In conventional, multi-shot imaging, an RF pulse is applied and the gradients are modulated, one RF pulse at a time,

to create the image. The number of RF pulse and gradient modulation pairs performed determines the y-resolution of the image. In EPI, the gradients are modulated (or switched) approximately the number of lines necessary to encode the image. Because the signal decays at a rate of $T2^*$ after the initial RF pulse, if the spatial encoding for an imaging plane is to be performed following a single RF pulse (i.e. with a single 'echo', hence the name 'echo-planar imaging'), it needs to be done very rapidly (otherwise the MRI signal will die away), therefore requiring rapidly switched gradients. With typical current technology, it takes approximately 25 to 40 ms to perform 64 spatial encoding steps. This limit is determined partially by physical limits of the scanner and by biological limits of the subject. If the rate of change of the magnetic field is too high, currents may be induced in the peripheral nerves, creating the sensation of 'twitching' which is not dangerous but can be painful.

Three methods exist for switching the gradients rapidly (Cohen and Weisskoff, 1991). One is to have extremely high-powered gradient amplifiers — a brute force approach. Another is to resonate the amplifier with the gradients, providing less flexibility in adjusting the gradient readout parameters. A third is to use a low-inductance gradient coil that does not require a large amount of power to create a rapidly switched and strong gradient. For imaging humans, the first systems were either the resonant type or standard clinical systems equipped with home-built low-inductance gradient coils. The use of local gradient coils, while cheap, does not offer much room for patients or for stimulus delivery. The introduction of EPI on clinical scanners — using the brute force high-powered gradient amplifier approach — was critical in the explosive growth in fMRI applications. This allowed users to simply buy a system for doing EPI rather than relying on the development of a system by a local team of physicists. Currently, hundreds of such systems are in operation, whereas, in 1992, only a small handful of centers could perform EPI.

Fig. 4 shows the prototype gradient coils used by the fMRI research lab at the Medical College of Wisconsin for 8 years on an otherwise standard clinical system (Wong, Bandettini and Hyde, 1992). Such a local gradient coil, designed and constructed by Eric Wong, currently of the University of Cal-

ifornia, San Diego, is also advantageous in that higher-gradient switching rates are achievable without inducing currents in peripheral nerves. Fig. 5 shows a 3 T General Electric scanner currently used at the NIH. It is equipped with whole-body gradients. Methods being developed to further increase gradient performance involve combining low-inductance gradient coil technology with high-powered gradient amplifiers. Using this technology, in combination with higher bandwidth receivers, and novel image encoding techniques based on multiple RF coil sensitivities, higher-resolution single-shot EPI will be possible. In addition, such applications such as diffusion tensor imaging will be possible in shorter amounts of time — a critical variable towards making such techniques ubiquitous in the clinic.

The last piece of technology discussed here is that of RF coils. Typically, for whole-brain imaging a quadrature 8 to 12 element coil is used. Most clinical RF coils are sensitive to signal from the entire head and upper neck area and are therefore sub-optimal for fMRI of the brain. Gains typically in the range of 30% in signal to noise can be obtained by using an RF coil that is closer to the head and has a reception field that does not extend beyond the base of the brain. One should be aware that, again, while gains in S/N of 30% are of course good, the temporal signal to noise is what really matters in functional MRI. At typical voxel volumes ($3 \times 3 \times 5 \text{ mm}^3$), a gain in 30% in signal to noise will likely translate to no more than a gain in about 10% in temporal signal to noise, given the presence of cardiac and respiratory fluctuations over time. At higher spatial resolutions, where thermal (or non-physiologic) noise dominates, gains in temporal contrast to noise will be more substantial with the use of more sensitive coils.

Surface coils have been typically used when imaging at very high resolution over a specific and highly localized region of interest, such as the visual or motor cortex. In this case, a small RF coil is placed over the region of interest. The signal to noise in this region is a function of the coil size, i.e. the smaller the coil, the greater the signal-to-noise ratio. A problem with surface coils is that they do not have a homogeneous reception or excitation field. This is a problem for reception in that the sensitivity drops off rapidly. It is a larger problem for excitation since the excitation energy is inhomogeneously

1991-1992



1992-1999

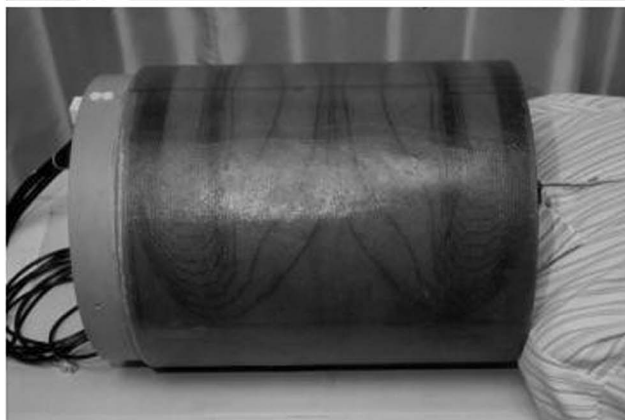


Fig. 4. Two versions of local head gradient coils, modeled by the author, and created by Eric Wong (currently at UCSD), used at the Medical College of Wisconsin. These low-inductance coils were necessary for performing echo-planar imaging on a standard clinical scanner (circa 1991–1998).

distributed, meaning that in one part of the brain, a 90° flip angle might be created, and 5 cm away, a 40° flip angle might be created. To create a homogeneous flip angle distribution, it is necessary to use either specialized excitation pulses or a larger coil for excitation. Typically, at 1.5 T, whole-body RF coils are typically used for excitation, therefore obviating this problem. At higher field strengths than 3 T, whole-body coils are not yet feasible. A workable strategy has been to use an intermediate-sized coil for excitation, and smaller coils inside the large coil for reception. In this case, a large excitation coil gives a homogeneous distribution of RF power and the surface receive coil focuses on a specific region for high-resolution and/or signal-to-noise fMRI.

Surface coils can be combined into arrays to increase signal-to-noise and brain coverage. In ad-

dition, specific pulse sequences involving RF sensitivity encoding are being designed to make use of independent surface coil arrays to increase signal to noise, imaging speed, image quality, and image resolution.

Pulse sequences

Functional MRI pulse sequences have developed along two paths. The first is towards the goal of obtaining the highest resolution and artifact free image as possible. The second is towards the goal of obtaining as specific and perhaps quantitative neuronal and/or physiologic information as possible. In this section, image acquisition strategies will first be discussed, and then information extraction methods will be described. In the section on information extrac-



Fig. 5. Clinical whole-body scanner with EPI capability. 3 T and EPI have become standard clinical products by most manufacturers after about 1998.

tion methods, a discussion on the major techniques will be given along with that of tradeoff issues and contrast sensitivity optimization issues.

Image quality and resolution

As mentioned above, the image acquisition rate is limited not only by how rapidly the imaging gradients can be switched and how rapidly the signal can be digitized but, for obtaining multiple images, it is also limited by the time it takes for protons to recover signal once they have been excited. MRI can be divided into single-shot and multi-shot techniques. In single-shot techniques, spins are excited with a single excitation pulse and all the data necessary for creation of an image are collected at once. Multi-shot techniques are the most commonly used method for high-resolution anatomical imaging. Usually, a single 'line' (in k-space) of raw data is acquired with each excitation pulse. Because of the relatively slow rate at which the magnetization returns to equilibrium following excitation (determined by the T1 of the tissue), a certain amount of time is required between shots; otherwise the signal would rapidly be saturated. Because of this required recovery time

(at least 150 ms), multi-shot techniques are typically slower than single-shot techniques. For a 150-ms TR, a fully multi-shot image with 128 lines of raw data would take $150 \text{ ms} \times 128 = 19.2 \text{ s}$.

In the case of echo-planar imaging, the entire data set for a single plane is typically acquired in about 20 to 40 ms. For an fMRI experiment, the TE is about 40 ms. Along with some additional time for applying other necessary gradients, the total time for an image to be acquired is about 60 to 100 ms, allowing 10 to 16 images to be acquired in a second. Improvements in digital sampling rates and gradient slew rates will allow further gains in this number, but essentially, this is about the upper limit for imaging humans.

In the context of an fMRI experiment with echo-planar imaging, the typical image acquisition rate is determined by how many slices can temporally fit into a TR time. For whole-brain imaging, approximately 20 slices (5 mm thickness) are required to cover the entire brain. This would allow a TR of about 1.25 to 2 s at minimum. This sampling rate is more than adequate to capture most of the details of the slow and dispersed hemodynamic response.

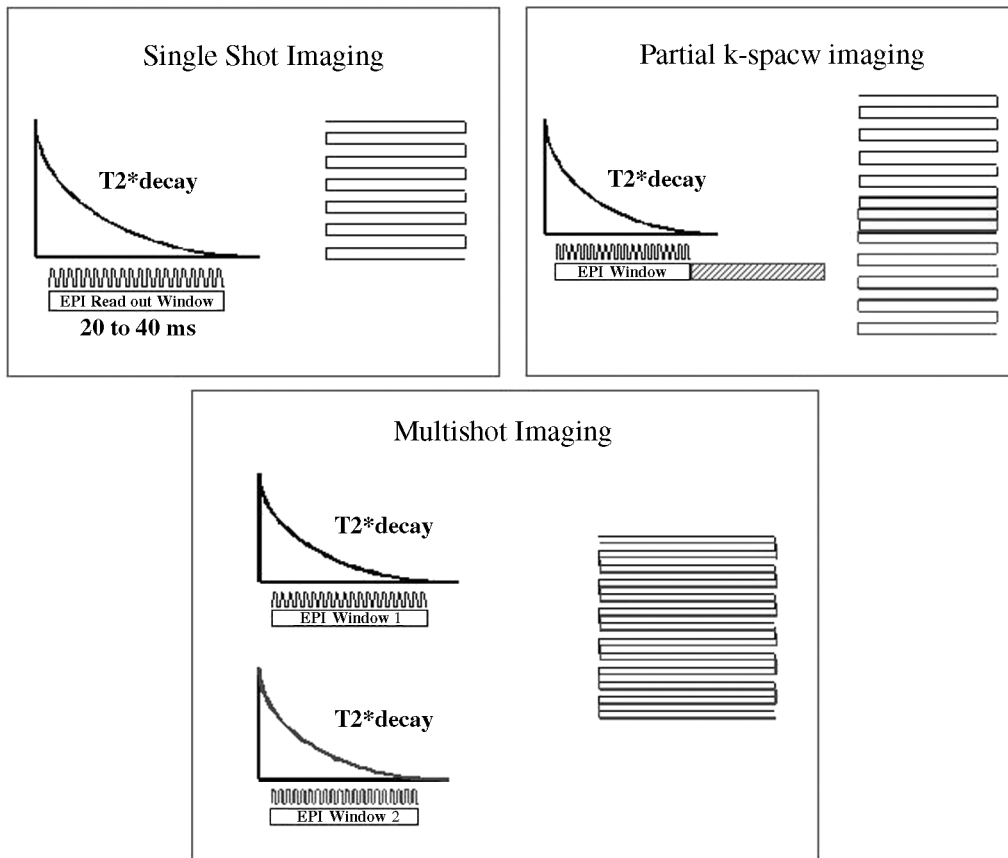


Fig. 6. Strategies for obtaining higher-resolution EPI. Top left depicts the standard single-shot EPI technique. Note that when the images are being collected, the signal is constantly decaying thus limiting the amount of useful sampling time. The strategy on the top right, conjugate synthesis, makes use of the redundancy of the k-space data to almost double the resolution in the phase encode direction. The strategy on the bottom is multi-shot EPI, which allows for double the resolution in the phase encode direction. The tradeoff is that the technique takes twice the time (two RF excitations) and sacrifices some temporal stability.

Image spatial resolution is also primarily determined by the gradient strength, the digitizing rate, and the time available. For multi-shot imaging, as high resolution as desired can be achieved if one is willing to wait: one can keep on collecting lines of data with more RF pulses. For single-shot EPI, the free induction decay time, T_2^* , plays a significant role in determining the possible resolution. One can only sample for so long before the signal has completely decayed. For this reason, echo-planar images are generally of lower resolution than multi-shot images. To circumvent the problem of decaying transverse signal, two strategies are commonly used (Cohen, 1999; Cohen and Weisskoff, 1991). The first strategy is multi-shot EPI, in which a larger k-space

data set is acquired in multiple interleaved passes (but still with many fewer passes than for conventional clinical multi-shot imaging). The second strategy is to perform an operation called conjugate synthesis, which involves making use of the fact that due to symmetry in the full k-space data, half of the data that conventionally is collected is redundant. By only measuring the minimum lines absolutely required, the uncollected lines of k-space can be calculated using the symmetry properties. This allows a gain of at most twice the spatial resolution in one direction, with some cost in signal-to-noise ratio and image quality (Jesmanowicz, Bandettini and Hyde, 1997). The procedure is also known as partial k-space EPI. These techniques are schematically shown in Fig. 6.

Multi-shot EPI suffers from some additional temporal stability problems that arise from the fact that the image acquisition takes longer than a complete cardiac cycle. In such a case, misalignment in k-space lines, sensitive to the phase of the cardiac cycle, can occur, creating ghosting that exists in each image and is variable from image to image due to variable sampling of the cardiac cycle. Navigator echoes, extra echoes used to help correct the phase errors that can occur with cardiac and respiratory pulsation, are somewhat effective in correcting these k-space misregistration problems. With partial k-space acquisition, the image quality tends to suffer because complete phase information for all k-space lines is not obtained. A further advantage of multi-shot EPI is that if the resolution is kept the same as with single-shot imaging, the effective readout echo intervals are shorter, reducing image distortion, which is proportional to the readout window width. This has been a way to work around the echo-planar image warping, and subsequent misregistration with higher-resolution image, problem to obtain a high-resolution multi-shot image with the same warping as a single-shot echo-planar image. Keeping the readout window the same width, and simply obtaining more lines in k-space by increasing the number of shots, is a way to do this.

Neuronal and physiologic information extraction

The second pulse-sequence development direction is along the direction of increasing the amount and quality of functional information that can be obtained from time series data.

Several types of physiologic information can be mapped using fMRI. This information includes baseline cerebral blood volume (Moonen, vanZijl, Frank et al., 1990; Rosen, Belliveau, Aronen et al., 1991; Rosen, Belliveau and Chien, 1989), changes in blood volume (Belliveau, Kennedy, McKinstry et al., 1991), baseline and changes in cerebral perfusion (Detre, Leigh, Williams and Koretsky, 1992; Edelman, Sievert, Wielopolski et al., 1994b; Kim, 1995; Kwong, Chesler, Weisskoff and Rosen, 1994; Williams, Detre, Leigh and Koretsky, 1992; Wong, Buxton and Frank, 1997), and changes in blood oxygenation (Bandettini et al., 1992; Frahm et al., 1992; Haacke, Lai, Reichenbach et al., 1997; Kwong et al., 1992; Ogawa and Lee, 1992; Ogawa, Lee, Kay

and Tank, 1990; Turner, LeBihan, Moonen et al., 1991). Recent advances in fMRI pulse sequence and experimental manipulation have allowed quantitative measures of oxygen extraction fraction (vanZijl, El-eff, Ulatowski et al., 1998), CMRO₂ changes data (Davis, Kwong, Weisskoff and Rosen, 1998b; Hoge, Atkinson, Gill et al., 1999a; Hoge, Atkinson, Gill et al., 1999b; Kim and Ugurbil, 1997) and dynamic non-invasive measures in blood volume (Liu, Luh, Wong et al., 2000) with activation to be extracted fMRI. Below, a quick overview of each technique is given. In addition, the issue of hemodynamic specificity is discussed.

Blood volume. In the late 1980s, the use of rapid MRI allowed tracking of transient signal intensity changes over time. One application of this utility was to follow the T2* or T2 weighted signal intensity as a bolus of an intravascular paramagnetic contrast agent passes through the tissue of interest (Rosen et al., 1989). As it passes through, susceptibility-related dephasing increases then decreases as the bolus washes out. The area under these signal attenuation curves are proportional to the relative blood volume. In 1990, Belliveau and colleagues took this one step further and mapped blood volume during rest and during activation (Belliveau et al., 1991). The first maps of brain activation using fMRI were demonstrated with this technique. As soon as the technique was demonstrated it was rendered basically obsolete (for brain activation imaging) by the use of an endogenous and oxygen-sensitive contrast agent: hemoglobin. Recently, non-invasive methods for dynamic measurement of blood volume have been suggested (Liu et al., 2000), yet due to signal-to-noise limitations, have not yet been implemented.

Blood oxygenation. As early as the 1930s it was known that deoxy-hemoglobin was paramagnetic and oxy-hemoglobin was diamagnetic (Pauling and Coryell, 1936). In 1982 it was discovered that changes in blood oxygenation changed the T2 of blood, but it was not until 1989 that this knowledge was used to image in vivo changes in blood oxygenation (Thulborn, Waterton, Matthews and Radda, 1982). Blood oxygenation level-dependent contrast, coined BOLD by Ogawa et al. (Ogawa et al., 1992), was used to image the activated brain for the first

time in 1991. The first results using BOLD contrast for imaging brain function were published in 1992 (Bandettini et al., 1992; Kwong et al., 1992; Ogawa et al., 1992). The basic concept behind this contrast mechanism is that with brain activation, a localized increase in blood flow causes an increase in blood oxygenation that exceeds metabolic need. Its presence of deoxy-hemoglobin in the blood causes $T2^*$ and $T2$ to be decreased. With the increase in blood oxygenation, and corresponding decrease in the amount of deoxyhemoglobin, $T2^*$ and $T2$ increase, leading to a small signal increase in $T2$ and $T2^*$ weighted images. Because of its sensitivity and the ease of implementation of gradient-echo ($T2^*$ weighted sequences) imaging, BOLD contrast using gradient-echo imaging has emerged to be the most commonly used fMRI method. Asymmetric spin-echo techniques, used extensively by one of the first groups to perform fMRI (Kwong et al., 1992), and having similar contrast as gradient-echo techniques, have been implemented.

Blood perfusion. An array of new techniques exists for mapping cerebral blood *perfusion* in humans. For a recent review, please refer to Wong (1999). Arterial spin-labeling-based perfusion mapping MRI techniques, abbreviated as ASL techniques, are conceptually similar to other modalities such as positron emission tomography (PET) and single photon emission computed tomography (SPECT) in that they involve tagging inflowing blood, and then allowing flow of the tagged blood into the imaging plane. The RF tagging pulse is usually a 180° pulse that ‘inverts’ the magnetization.

These techniques can be subdivided into those which use continuous arterial spin labeling, which involves continuously inverting blood flowing into the slice, and those that use pulsed arterial spin labeling, which involves periodically inverting a block of arterial blood and measuring the arrival of that blood into the imaging slice. Examples of these techniques include ‘echo-planar imaging with signal targeting and alternating RF’ (EPSTAR) (Edelman, Siewert and Darby, 1994a) and ‘flow-sensitive alternating inversion recovery’ (FAIR) (Kim, 1995; Kwong, Chesler, Weisskoff et al., 1995). Recently, a pulsed arterial spin labeling technique known as ‘quantitative imaging of perfusion using a single

subtraction’ (QUIPSS) has been introduced (Wong, Buxton and Frank, 1998).

Hemodynamic specificity. With each of the above-mentioned techniques for imaging volume, oxygenation, and perfusion changes, the precise type of observable cerebrovascular information can be more finely delineated. While this information, described below, is typically more than most fMRI users are primarily concerned about, it is useful to have an abbreviated summary of how specific MRI can be. Please refer to Fig. 7 for a schematic depiction of pulse sequence sensitization to specific vascular components and the heterogeneity of the vasculature across voxels. It shows intravascular and extravascular signal. If the specific vessel type is filled in (either red: arteries; or blue: veins), then there exists a contribution from intravascular effects. If the region around the vessel is filled in, then there extravascular spins (exchanging spins — with ASL, and extravascular gradients — with BOLD) contribute to the functional contrast. Regarding susceptibility contrast imaging, spin-echo sequences are more sensitive to small susceptibility compartments (capillaries and red blood cells) and gradient-echo sequences are sensitive to susceptibility compartments of all sizes (Bandettini and Wong, 1995; Boxerman, Hamberg, Rosen and Weisskoff, 1995b; Kennan, Zhong and Gore, 1994; Ogawa, Menon, Tank et al., 1993; Weisskoff, Boxerman, Zuo and Rosen, 1993). A common mistake is to assume that spin-echo sequences are sensitive to capillaries only. Since red blood cells also are also ‘small compartments’, spin-echo sequences are selectively sensitive to intravascular signal arising from small *and large* vessels (Boxerman, Bandettini, Kwong et al., 1995a). Since BOLD contrast is highly weighted by the resting state blood volume that happens to be in the voxel, it is likely that many voxels having pial vessels running through them will have at least 50% blood volume. These voxels are therefore likely to show the largest gradient-echo *and spin-echo* signal changes. At field strengths of 9 T or above, intravascular spins may no longer contribute since the $T2^*$ and $T2$ of blood becomes extremely short (Lee et al., 1999).

Outer volume RF saturation removes inflowing spins (Duyn, Moonen, van Yperen et al., 1994), therefore reducing non-susceptibility-related inflow

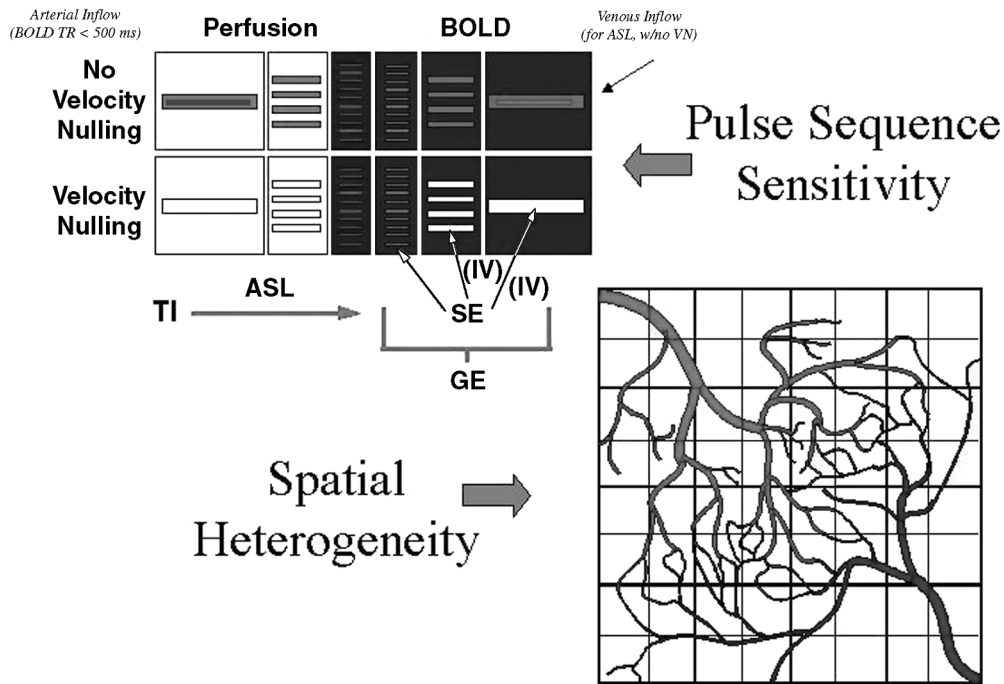


Fig. 7. Diagram showing the vascular tree and the spatial heterogeneity of the vasculature over space. An important point is that many of the hemodynamic variables that influence BOLD contrast vary considerably from voxel to voxel. The pulse sequences (ASL, arterial spin labeling; TI, inversion time), (GE, gradient echo; SE, spin echo) and their manipulations (velocity nulling — basically the addition of diffusion gradients) can sensitize the signal to specific aspects of the vascular tree when used to observe hemodynamic changes with brain activation. A challenge is that as the sequences become more sensitized to capillaries exclusively, the signal to noise (and therefore functional contrast to noise) drops significantly. Most users put up with the sensitivity across different blood pools in order to maximize functional contrast to noise.

changes when using short TR (with high flip angle) sequences. Diffusion weighting or ‘velocity nulling’, involving the use of $b > 50 \text{ s}^2/\text{mm}$, effectively dephases rapidly moving intravascular signal (Boxerman et al., 1995a) therefore reducing, but not eliminating, large vessel effects (intravascular effects are removed but extravascular effects remain) in gradient-echo fMRI and all large vessel effects in spin-echo fMRI. A significant caveat in this approach is that, at 1.5 T, application of this amount of diffusion weighting reduces BOLD signal by about 60% (Boxerman et al., 1995a) which is prohibitive under even the most optimal circumstances. This also implies that, at 1.5 T, up to 60% of the BOLD signal comes from intravascular signal and not from protons in tissue experiencing modulation of magnetic field gradients around vessels.

Performing BOLD contrast fMRI at high field strengths has the same effect as diffusion weight-

ing in the context of susceptibility-based contrast because the $T2^*$ and $T2$ of venous blood becomes increasingly shorter than the $T2^*$ and $T2$ of gray matter as field strength increases, therefore less signal will arise from intravascular space at higher field strengths (Menon et al., 1993). This unique characteristic of imaging at high field strengths can be put to use in the creation of high-resolution venograms (Menon et al., 1993). An example of a high-resolution venogram created at 3 T (courtesy of S. Casciaro and Z. Saad) is shown in Fig. 8. This particular display is a minimum intensity projection of simply a $T2^*$ weighted multi-shot sequence.

Mapping of $CMRO_2$. Recently, advances in mapping activation-induced changes in the cerebral metabolic rate of oxygen ($CMRO_2$) using fMRI have developed (Davis et al., 1998b; Hoge et al., 1999a,b; Kim, Rostrup, Larsson et al., 1999). The basis for such

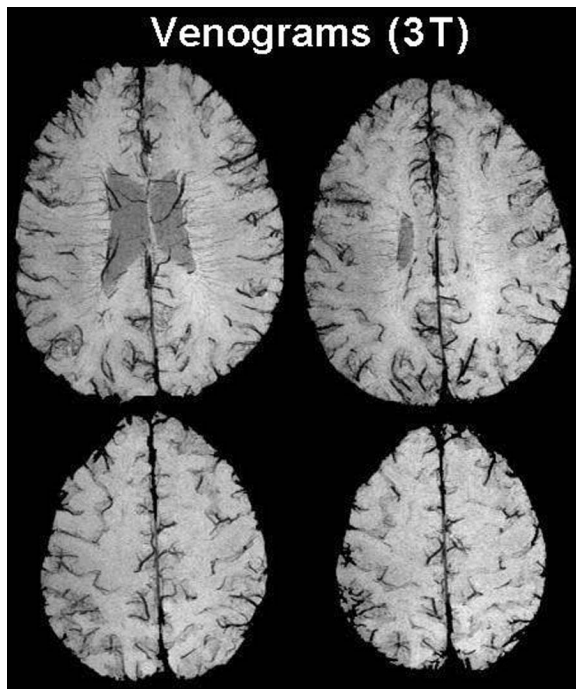


Fig. 8. High-resolution venograms. 3D T_2^* weighted sequence. The display is a minimum intensity projection across about 5 1-mm-thick slices. (Axial 3D, SPGR, Flow compensated, TE = 30 ms, TR = 50 ms, Flip angle = 20 degrees, FOV 22, Thickness: 1 mm, 512×256 , 1 NEX.) These images show veins (dark) independent of flow velocity. Because blood T_2^* is shorter than gray matter T_2^* at field strengths of 3 T and higher, one simply needs to collect a T_2^* weighted image. Collection in 3D mode substantially improves signal to noise, and the use of minimum intensity projection (a feature of AFNI) improves delineation of the veins. Of course, other sources of field inhomogeneities on the spatial scale of veins can lead to some misinterpretation. (Courtesy of S. Casciaro and Z. Saad.)

inferences is that BOLD and perfusion contrast can be explained by the combination of a handful of parameters. The number of unknown parameters can be reduced, using the appropriate pulse sequence selection, or the physiologic state can be manipulated. Normalization or calibration using a hypercapnia stress has evolved to be a method for reducing the number of unknown parameters to allow for mapping of changes in $CMRO_2$ (Davis et al., 1998b). The basic concept here is that when the brain is activated, increases in flow, volume, and oxygenation are accompanied by an increase in $CMRO_2$. When a subject at rest is undergoing a hypercapnic stress (5% CO_2), the cerebral flow, volume, and oxygena-

tion increase without and accompanying increase in $CMRO_2$, therefore less oxygen is extracted from the blood, allowing the blood oxygenation change, relative to the perfusion change, to be greater than with brain activation. By comparing the ratio of the (simultaneously measured) perfusion and BOLD signal changes during hypercapnia and during brain activation, $CMRO_2$ information can be derived.

Methods for extraction of baseline $CMRO_2$ are on the immediate horizon (An, Lin, Celik and Lee, 2001). The key to these techniques is the more precise extraction of hemodynamic information, such as blood volume and blood oxygenation, and the use of appropriate calibration procedures.

Tradeoffs of each technique. Table 2 summarizes the practical tradeoffs involved with the use of each of the above-mentioned types of sequences for information extraction.

With BOLD contrast, several distinct advantages exist. First, it is of course, completely non-invasive. Second, the functional contrast to noise is at least a factor of 2 to 4 greater than that of perfusion imaging. Third, it is easiest to implement since it only requires, typically, a gradient-echo sequence with an echo time (TE) = 30 to 40 ms. Fourth, it is nearly trivial to perform multi-slice whole-brain echo-planar imaging (EPI). All that is required is that the repetition time (TR) is long enough to accommodate all of the slices in each volume. Typically, with a TE of about 40 ms, the total time for acquiring a single-shot echo-planar image is about 60 to 100 ms, which translates to a rate of 10 to 16 slices per second. If a reduced number of slices is allowed, then a very short TR can be utilized for fine temporal mapping of the dynamics of the BOLD signal change.

Several disadvantages exist in regard to BOLD contrast imaging. First, as is described above, BOLD contrast is extremely complicated, involving the interplay of perfusion, $CMRO_2$, and volume changes, and modulated by the heterogeneity of the vasculature and neuro-vascular coupling over time and space. This problem leads to limits of interpretation of the location, magnitude, linearity, and dynamics of BOLD contrast signal. In addition, it makes across-population comparisons, clinical mapping, and pharmacologic effect mapping extremely

TABLE 2

Summary of the practical advantages and disadvantages of pulse sequences that have contrast based on BOLD, perfusion, volume, and CMRO₂

	Advantages	Disadvantages
BOLD	<ul style="list-style-type: none"> – highest functional activation contrast by a factor of 2 to 4 over perfusion – easiest to implement – multi-slice trivial – can use very short TR 	<ul style="list-style-type: none"> – complicated non-quantitative signal – no baseline information – susceptibility artifacts
Perfusion	<ul style="list-style-type: none"> – unique and quantitative information – baseline information – easy control over observed vasculature – non-invasive – no susceptibility artifacts 	<ul style="list-style-type: none"> – low functional activation contrast (up to 7 T) – longer TR required – multi-slice is difficult – slow mapping of baseline information
Volume	<ul style="list-style-type: none"> – unique information – baseline information – multi-slice is trivial – rapid mapping of baseline information 	<ul style="list-style-type: none"> – invasive – susceptibility artifacts – requires separate rest and activation runs
CMRO ₂	<ul style="list-style-type: none"> – unique and quantitative information 	<ul style="list-style-type: none"> – semi-invasive (requires CO₂ inhalation) – low functional activation contrast – susceptibility artifacts – processing intensive – multi-slice is difficult – longer TR required

challenging. Also, unlike the perfusion and volume mapping methods, no baseline oxygenation information can, yet, be obtained since resting state T2* and T2 times are dominated by tissue type rather than oxygenation state. Progress is being made though (Yablonskiy, 1998). If resting state oxygenation information is implied, considerable assumptions have to be made regarding blood volume and vessel geometry, among other things. Another problem with BOLD contrast in general is that the same susceptibility weighting that allows for the observation of the functional contrast also contributes to many of the artifacts in the images used. These artifacts include signal dropout at tissue interfaces and at the base of the brain. The problem becomes greater at higher field strengths.

The advantages of perfusion contrast make it useful for specific studies requiring a more calibrated signal, but is generally less robust than BOLD contrast for cognitive brain activation mapping. The first advantage is that quantitative maps of perfusion changes can be obtained. The changes in signal are simply due to perfusion changes and not based on any complicating interactions of neurovascular cou-

pling and volume dynamics. Also, quantitative maps of resting state or baseline perfusion are obtained in every time series as well. With modulation of the timing parameters such as the inversion time (TI), specific parts of the vasculature may be isolated based on their flow rates. Since the tag of inflowing spins involves only the use of an RF pulse, the technique is non-invasive. Lastly, since the basis of the contrast is not susceptibility, an extremely short TE can be used, significantly reducing susceptibility artifacts. For this reason, this technique might be the method of choice for mapping activation near the problematic tissue interfaces and at the base of the brain.

Perfusion imaging has several potentially prohibitive disadvantages. First, the functional contrast to noise is lower than BOLD contrast by a factor of about 2 to 4, at field strengths below 3 T, leading to the requirement of more temporal averaging (by a factor of 4 to 16) to achieve similar quality activation maps. Second, because of the time required to allow the tagged blood to perfuse into the tissue of interest (TI), a relatively long TR is required. The minimum TR that is used is typically 2 s. Nevertheless, tech-

niques are emerging that allow for a shorter TR to be used (Duyn, Tan, van der Veen et al., 2000; Liu and Gao, 1999; Wong, Luh and T, 2000) or that allow the user to work around the long TR problem (Buxton, Wong and Frank, 1998b; Buxton, Luh, Wong et al., 1998a) by using periodically divisible TR and the stimulus timing intervals. Third, because the tagged spins undergo a decaying of signal (dictated by the T1 of blood), all the images have to be acquired in a very short time, putting a limit on the number of slices obtained. In addition, each slice has a different TI associated with it, making quantification slightly more difficult. The typical upper limit of slices is in the range of 5 to 10. Lastly, in a clinical setting where mapping of baseline perfusion information may be critical, ASL requires more time to create a usable map than the blood volume mapping (perfusion information can be derived from transit time) technique that has been used clinically. For mapping baseline information, ASL is slower than blood volume mapping by a factor of at least 3, which is potentially critical when determining compromised perfusion in acute stroke for instance.

Blood volume mapping has the same advantage as ASL in that the information derived is unique, and that baseline information of blood volume and perfusion (which can be derived by taking into consideration the measured transit time) can be obtained. It has all the advantages of BOLD in that multi-slice imaging is trivial and a very short TR can be used if desired. As mentioned above, baseline information can be mapped at least twice as fast as with ASL techniques.

Blood volume mapping with a bolus injection of a susceptibility contrast agent has its drawbacks. Even though the contrast agents are nontoxic at the doses given, the technique is considered invasive. Larger doses or repeated doses become toxic. All brain activation maps obtained with this technique have involved separate runs of about 2 min each: the first being a rest state and the second an activated state. Since the number of repeated doses is limited, a limit is placed on what types of cognitive questions can be asked with the use of this technique. Because of the limited number of brain activation studies performed with this technique, it is difficult to draw a conclusion regarding its relative functional activation contrast to noise.

CMRO₂ change mapping is still a work in progress. Its big potential is that the information is unique and perhaps most associated with neuronal activity. Of course, to derive this information, several still-unresolved assumptions about the hemodynamic changes with a CO₂ stress and about the perfusion and BOLD signal itself have to be made.

Since this method for mapping CMRO₂ changes uses techniques that simultaneously map perfusion and BOLD, it has all of the disadvantages of both techniques, and at least one more. The additional disadvantage is that it typically requires the subject to breathe a gas mixture of elevated CO₂ for a duration of at least 2 min. This is slightly uncomfortable for the motivated volunteer and may even be lethal to a patient.

Sensitivity. Extraction of a 1–5% signal change against a backdrop of thermal noise, physiologic fluctuations, motion, and system instabilities requires careful consideration of the variables which influence signal detectability. These range from factors that optimize fMRI contrast, increase signal, reduce physiologic fluctuations, and minimize artifactual signal changes.

Contrast optimization. With regard to BOLD contrast, gradient-echo (or asymmetric spin-echo) sequences are typically used because they produce the largest activation-induced signal changes by a factor of 2 to 4 over other contrast sensitizations. Gradient-echo images are collected during the free induction decay of the signal after an initial RF pulse is applied. This decay can be described by a signal exponential function with a decay rate = $1/T_2^*$ or a decay time of T_2^* . During activation, this decay rate decreases slightly. The TE that optimizes contrast when performing gradient-echo fMRI is that which maximizes the difference between two exponential decay rates (T_2^* during rest and T_2^* during activation). This maximization occurs at $TE \approx \text{resting } T_2^*$ (Bandettini, 1995). When performing spin-echo fMRI, since changes in T_2 are observed, the optimal $TE = \text{resting } T_2$. While the percent signal change increases linearly with TE, the contrast — what matters — has a well-defined peak at $TE \approx \text{resting } T_2^*$.

With asymmetric spin-echo sequences, BOLD contrast is optimized when the image is collected

at a time, τ , from the spin-echo. To maximize BOLD contrast, τ should also be approximately equal to $T2^*$ of the tissue. Asymmetric spin-echo sequences require more time per slice than gradient-echo sequences, but are moderately less sensitive to pulsatile flow-related fluctuations.

?#1

With arterial spin labeling, the typical goal is to tailor the shape and of the tagged blood such that the tagged blood only perfuses the tissue of interest and does not flow through. This goal is to optimize quantification or information content (Wong, 1999; Wong et al., 1998). Maps having greater functional contrast, but also contain blood which is flowing through the tissue, can be created without the necessary controls for quantification, improving signal to noise by at least a factor of 2.

While not directly improving perfusion contrast itself, ways for improving signal to noise without compromising quantification include the use of as short of a TE as possible. In single shot imaging, starting at the center of k-space, as with spiral imaging, allows for an extremely short TE (as short as 3 ms), allowing for higher signal to noise (Glover and Lee, 1995; Noll, Cohen, Meyer and Schneider, 1995).

Methods exist that are able to collect both BOLD contrast and perfusion contrast in a single run. These include techniques that collect perfusion and BOLD during separate segments of the run (Hoge et al., 1999a), those that use the same images for perfusion and BOLD contrast calculations (Wong and Bandettini, 1999), and those that employ a double echo sequence, using the first echo (short TE: no $T2^*$ weighting) for optimally obtaining perfusion information and the second echo (long TE: high $T2^*$ weighting) for optimally obtaining BOLD information.

Methodology

Methodology is used here as meaning the strategies by which the technology and the understanding of the signal is brought to bear towards specific applications. While this definition can be quite broad, covering everything including subject handling, subject interface, data processing, and data pooling, the focus in this section will primarily be on how neuronal activation paradigms can be designed. A

Neuronal Activation Input Strategies

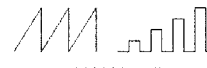
1. Block Design 
2. Parametric Design 
3. Frequency Encoding 
4. Phase Encoding 
5. Event Related 
6. Orthogonal Design 
7. Free Behavior Design 

Fig. 9. Neuronal activation input strategies. These schematically depict the methods by which neuronal activation can be played out over time in a single time series. The neuronal activation input strategies are closely tied to the processing methods and with the specific questions being asked.

schematic summary of these strategies is shown in Fig. 9. A description of each of these is given below.

Block design

A block design paradigm was the first used in fMRI and is still the most prevalent neuronal input strategy. Essentially adapted from positron emission tomography paradigm designs, it involves having a subject perform a task for at least 10 s (to reach hemodynamic steady state, discussed below), alternated for a similar time with one or multiple control tasks. This is a useful technique in that it is easy to implement and standard statistical tests can be used to compare each condition.

Parametric designs

The use of parametric designs appeared almost immediately following block designs. One of the first experiments performed, once it was observed that the fMRI signal increased with activation, was to vary the intensity of activation and characterize how the response differentially tracks the intensity of activation in different regions of the brain (Binder, Rao, Hammeke et al., 1994; Rao, Bandettini, Binder et al., 1996; Kwong et al., 1992). The essential aspect of

parametrically designed tasks is that the task itself is varied in some systematic fashion and the corresponding changes in the brain are compared rather than simply the magnitudes themselves against a single control task. The results from tasks such as these are more directly interpretable in that if only two conditions are compared, the magnitude of activation is highly influenced by the resting venous blood volume in each voxel. When the task is systematically varied, and the slopes compared on a voxel-wise basis, the spatial variations in blood volume and other physiologic factors not related to brain activation are controlled for to some degree. Parametric designs can involve continuous variation of the stimuli or can be set up in a blocked fashion, with each block involving a different degree or intensity of stimulation.

Frequency encoding

Frequency encoding is probably the least common of task designs, but perhaps lends itself optimally to very specific types of stimuli. The method involves designating a specific on–off frequency for each type of stimulus used. Again, the use of Fourier analysis to analyze the data reveals the most power under a specific spectral peak corresponding to the brain area specific to the particular on–off frequency. The utility of this method has been demonstrated in the mapping of left and right motor cortex by cueing the subject to perform a finger-tapping task at different on–off rates for each hand (Bandettini, 1995; Bandettini, Jesmanowicz, Wong and Hyde, 1993). In general, the goal of any paradigm design is to encode as much information as possible into a single time series. This allows more precise comparisons since a primary source of error is variation across time series due to scanner instabilities or subject movement. Keeping as many comparisons as possible in one time series is a method to reduce the effects of these variations.

Phase encoding

Phase encoding the stimulus input involves varying some aspect of the stimuli in a continuous and cyclic manner. This strategy has been most successfully used in performing retinotopic mapping (DeYoe, Carman, Bandettini et al., 1996; Engel, Glover and

Wandell, 1997; Sereno, Dale, Reppas et al., 1995). In this type of study, a visual stimulus ring is continuously varied in eccentricity, then, after the most extreme eccentricity is reached, the cycle is repeated again. The data are then typically analyzed using Fourier analysis, mapping out the areas that show a signal change temporal phase that correlates with the stimulus phase. This is a powerful technique since it makes use of the entire time series in that there are no ‘off’ states. It also lends itself to Fourier analysis — a powerful analysis technique. This method has also been used for somatotopic mapping (Servos, Zacks, Rumelhart and Glover, 1998), and tonotopic mapping (Talavage, Ledden, Sereno et al., 1996).

Event-related designs

Before 1995, a critical question in event-related fMRI was whether a transient cognitive activation could elicit a significant and usable fMRI signal change. In 1996, Buckner et al. demonstrated that, in fact, event-related fMRI lent itself quite well to cognitive neuroscience questions (Buckner, Bandettini, O’Craven et al., 1996). In their study, a word stem completion task was performed using a ‘block-design’ strategy and an event-related strategy. Robust activation in the regions involved with word generation were observed in both cases.

Given the substantial amount of recent publications which use event-related fMRI (Bandettini and Cox, 2000; Belin, Zatorre, Hoge et al., 1999; Birn, Bandettini, Cox and Shaker, 1999; Buckner, 1998; Buckner, Koutstaal, Schacter et al., 1998b; Buckner, Goodman, Burock et al., 1998a; Burock, Buckner, Woldorff et al., 1998; Clare, Humberstone, Hykin et al., 1999; Constable, Carpentier, Pugh et al., 2000; Dale, 1999; Davis, Kwan, Crawley and Mikulis, 1998a; D’Esposito, Postle, Ballard and Lease, 1999a; D’Esposito, Postle, Jonides and Smith, 1999b; D’Esposito, Zarahn and Aguirre, 1999c; Friston, Josephs, Rees and Turner, 1998b; Friston, Fletcher, Josephs et al., 1998a; Friston, Zarahn, Josephs et al., 1999; Glover, 1999b; Josephs, Turner and Friston, 1997; Josephs and Henson, 1999; Kang, Constable, Gore and Avrutin, 1999; Kiehl, Liddle and Hopfinger, 2000; McCarthy, 1999; Pinel, Le Clec, van de Moortele et al., 1999; Postle and D’Esposito, 1999; Rosen, Buckner and Dale, 1998;

Schacter, Buckner, Koutstaal et al., 1997; Schad, Wiener, Baudendistel et al., 1995), it can be probably said that this is one of the more exciting developments in fMRI since its discovery.

The advantages of event-related activation strategies are many (Zarahn, Aguirre and D'Esposito, 1997). These include the ability to more completely randomize task types in a time series (Clark, Maisog and Haxby, 1998; Dale and Buckner, 1997a; McCarthy, Luby, Gore and Goldman-Rakic, 1997), the ability to selectively analyze fMRI response data based on measured behavioral responses to individual trials (Schacter et al., 1997), and the option to incorporate overt responses into a time series. Separation of motion artifact from BOLD changes is possible by the use of the temporal response differences between motion effects and the BOLD contrast-based changes (Birn et al., 1999).

When using a constant ISI, the optimal ISI is about 10 to 12 s. Dale and Buckner (1997b) have shown that responses to visual stimuli, presented as rapidly as once every 1 s, can be adequately separated using overlap correction methods. Overlap correction methods are only possible if the ISI is varied during the time series. These results appear to demonstrate that the hemodynamic response is sufficiently linear, or at least additive, to apply deconvolution methods to extract overlapping responses. Burock et al. (1998) has demonstrated that remarkably clean activation maps can be created using an average ISI of 500 ms. Assuming the hemodynamic response is essentially a linear system, there appears to be no obvious minimum ISI when trying to estimate the hemodynamic response. Dale has suggested that an exponential distribution of ISIs, having a mean as short as psychophysically possible, is optimal for estimation (Dale, 1999). Of course the fastest one can present stimuli depends on the study being performed. Many cognitive tasks may require a slightly longer average presentation rate.

Recent work by Birn, Cox and Bandettini (2002) and Liu, Frank, Wong and Buxton (2001) has determined the optimal timing parameters to use when performing variable ISI event-related studies. It turns out that the optimal design depends on the question being asked. If one is interested in simply making the most robust map of activation, the longer the stimulation duration the better, and the optimal ISI is such

that the average ISI is the stimulus duration, resulting in a 50/50 distribution of on vs. off time. If one is interested in creating the most accurate estimate of the hemodynamic response — say for comparisons of subtle changes in activation in a predetermined region — then the shorter the task duration the better. Aside from that the same rules apply. A 50/50 distribution of on vs. off time is optimal. These two strategies result in extremely different optimization curves, as shown in Figs. 10 and 11.

?#2

Orthogonal designs

Orthogonal task design is a powerful extension of block design studies. The basic concept is that if one designs two different task timings that would create BOLD responses that are orthogonal to each other (i.e. their vector product is zero), then these tasks can be performed simultaneously during a single time series collection with no cross-task interference, making comparison much more precise. This technique was first demonstrated by Courtney, Ungerleider, Keil and Haxby (1997). In their study, six orthogonal tasks were designed into a single time series. This type of design also lends itself to event-related studies.

Free behavior designs

For many types of cognitive neuroscience questions, it is not possible to precisely constrain the timing or performance of a task. It is necessary then to allow the subject to perform the task 'freely' and take a continuous measurement of the performance, then use this measurement as a reference function for subsequent time series analysis. Examples of this type of design are emerging. As an example, the skin conductance changes are difficult to predict or control. In a study by Patterson, Bandettini and Ungerleider (2000), skin conductance was simultaneously recorded during an array of tasks and during 'rest'. The skin conductance signal change was then used as a reference function in the fMRI time series analysis. Several cortical and subcortical regions were shown to have signal changes that were highly correlated with the skin conductance changes. Without the use of this measurement, these signal changes would appear as noise. It is thought that

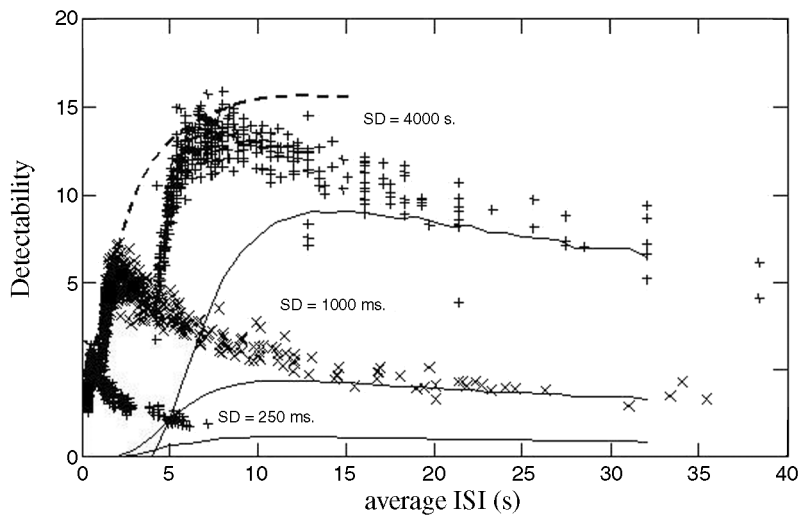


Fig. 10. Detectability (essentially the ability to make a statistical map) vs. average ISI for stimuli with varying ISI (points and dashed line) and constant ISI (solid lines) for 3 different minimum stimulus durations: 1000, 2000, and 4000 ms. Stimulus patterns with larger minimum stimulus durations (SD) are more similar to blocked designs, varying more slowly between task and control states. Detectability increases with larger minimum stimulus durations. (Adapted from Birn et al., 2002.)

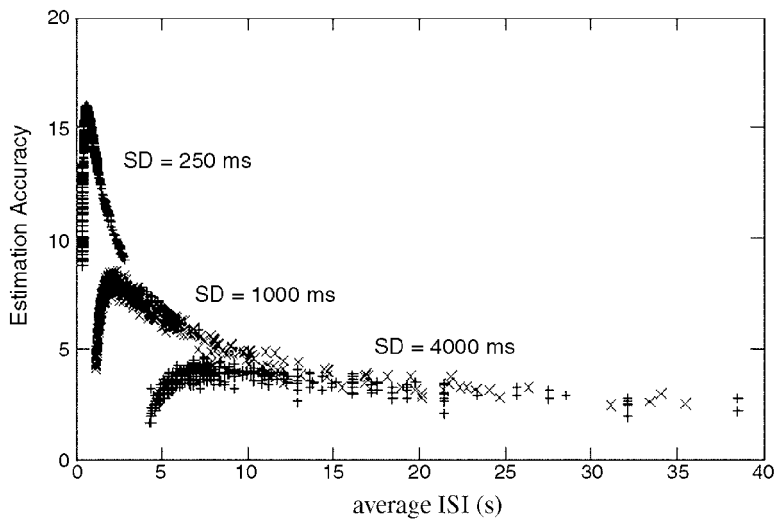


Fig. 11. Estimation accuracy (essentially the ability to characterize the hemodynamic response from a pre-defined region) vs. average ISI for stimuli with varying ISI (points and dashed line) for 3 different minimum stimulus durations: 1000, 2000, and 4000 ms. Stimulus patterns with larger minimum stimulus durations (SD) are more similar to blocked designs, varying more slowly between task and control states. Estimation accuracy increases with smaller minimum stimulus durations. (Adapted from Birn et al., 2002.)

this type of design will become more prevalent as methods to precisely monitor subject performance or state become more sophisticated.

Interpretation

For many users, the issues involved with determining the precise neural underpinnings of BOLD contrast may seem a esoteric after more than 10 years of

successful implementation of fMRI. It is clear that changes in BOLD contrast-derived maps, for the most part, correlate well with maps derived using other techniques. BOLD is successful for these reasons. While the success of BOLD contrast has of course allowed new insights into to be human brain function to be derived, the technique can certainly have much more potential in regard to spatially resolved quantitation of neuronal activity. We, as users, would love to use it for ever more applications: more precise comparison of subject populations, parametric manipulations, and extraction of transient neuronal activity; better understanding networked activity, understanding coupling variations in disease and healthy subjects, and for deriving maps of resting state activity.

In this section, the specific characteristics, including location, latency, magnitude, and linearity of the fMRI signal will be described in more detail. Emphasis will be placed on the how this understanding relates to practical implementation of fMRI.

Location

In resting state, hemoglobin oxygen saturation is about 95% in arteries and 60% in veins. The increase in hemoglobin saturation with activation is largest in veins, changing in saturation from about 60% to 90%. Likewise, capillary blood changes from about 80% to 90% saturation. Arterial blood, already saturated, shows no change. This large change in saturation is one reason why the strongest BOLD effect is usually seen in draining veins.

The second reason why the strongest BOLD effect is seen in draining veins is that activation-induced BOLD contrast is highly weighted by blood volume in each voxel. Since capillaries are much smaller than a typical imaging voxel, most voxels, regardless of size, will likely have about 2% to 4% capillary blood volume. In contrast, since the size and spacing of draining veins is on the same scale as most imaging voxels, it is likely that veins dominate the relative blood volume in any voxel that they pass through. Voxels that pial veins pass through can have 100% blood volume while voxels that contain no pial veins may have only 2% blood volume. This stratification in blood volume distribution strongly determines the magnitude of the BOLD signal.

As suggested in Fig. 7, different pulse sequence weightings can result in different locations of activation. For instance, in regard to imaging perfusion and BOLD contrast, while much overlap is seen, the hot spots vary by as much as 10 mm. The perfusion change map is sensitive primarily to *capillary* perfusion changes, while the BOLD contrast activation map is weighted mostly by veins. A potential worry regarding fMRI location is that venous blood, flowing away from the activated area, may maintain its elevated oxygen saturation as far as a centimeter away. When observing brain activation on the scale of centimeters, this has not been a major concern. Nevertheless this issue will be discussed in detail later in the chapter.

Latency

One of the first observations made regarding fMRI signal changes is that, after activation, the BOLD signal takes about 2 to 3 s to begin to deviate from baseline (Bandettini, 1993; Frahm et al., 1992). Since BOLD signal is highly weighted towards venous oxygenation changes, with a flow increase, the time for venous oxygenation to begin to increase will be about the time that it takes blood to travel from arteries to capillaries and draining veins, i.e. 2 to 3 s. The hemodynamic ‘impulse response’ function has been effectively used to characterize much of the BOLD signal change dynamics (Cohen, 1997; Friston et al., 1998b; Josephs et al., 1997). This function has been empirically derived by performing very brief and well-controlled stimuli. In addition it can be derived by deconvolving the neuronal input from the measured hemodynamic response (Dale and Buckner, 1997b; Glover, 1999b). This type of analysis assumes that the BOLD response behaves in a manner that can be completely described by linear systems analysis, which is still an open issue. Regardless, observed hemodynamic response to any neuronal activation can be predicted with a reasonable degree of accuracy, by convolving expected neuronal activity timing with the BOLD ‘impulse response’ function. This function has typically been mathematically described by a Gamma Variate function (Cohen, 1997).

If a task onset or duration is modulated, the accuracy to which one can correlate the modulated input

parameters to the measured output signal depends on the variability of the signal within a voxel or region of interest. In a study by Savoy, O'Craven, Weisskoff et al. (1994) addressing this issue, variability of several temporal sections of an activation-induced response were determined. Six subjects were studied, and for each subject, ten activation-induced response curves were analyzed. The relative onsets were determined by finding the latency with which the correlation coefficient was maximized with each of three reference functions, representing three parts of the response curve: the entire curve, the rising section, and the falling section. The standard deviation of the whole curve, rising phase, and falling phase were found to be 650 ms, 1250 ms, and 450 ms, respectively (Savoy, Bandettini, Weisskoff et al., 1995).

Across-region and within-region variations in the onset and return to baseline of the BOLD signal during primary visual activation (Saad, Ropella, Cox and DeYoe, 2001) and cognitive tasks have been observed (Buckner et al., 1996). For example, during a visually presented event-related word stem completion task Buckner et al. (1996) reported that the signal in visual cortex increased about 1 s before the signal in the left anterior prefrontal cortex. One might argue that this observation makes sense from a cognitive perspective since the subject first observes the word stem, then, after about a second, generates a word to complete this task. Others would argue that the neuronal onset latencies should not be more than about 200 ms. Can inferences of the cascade of brain activation be made on this time scale from fMRI data? Without a method to constrain, or work around the intrinsic variability of the onset of BOLD signal over space, such inferences should not be made in temporal latency differences below about 4 s.

Lee and Glover were the first to observe that the fMRI signal change onset within the visual cortex during simple visual stimulation varied from 6 s to 12 s (Lee, Glover and Meyer, 1995). These latencies were also shown to correlate with the underlying vascular structure. The earliest onset of the signal change appeared to be in gray matter and the latest onset appeared to occur in the largest draining veins. Similar latency dispersions in motor cortex have been observed. In one study, latency differences, detected in visual cortex using the Hilbert transform,

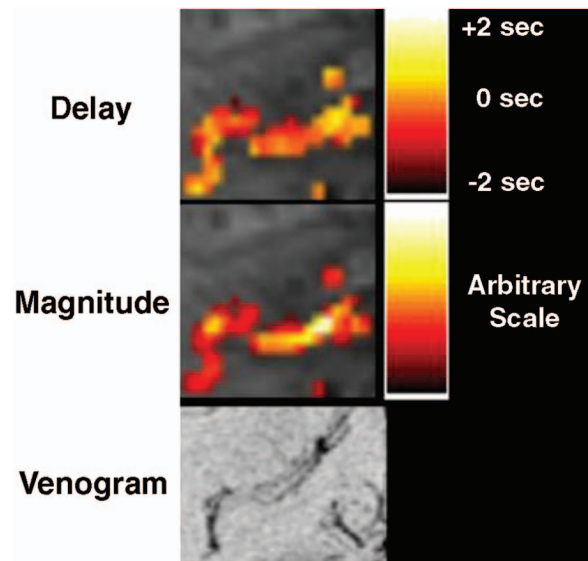


Fig. 12. Maps of activation latency and magnitude in the primary motor cortex during a finger-tapping task. The bottom of the image shows a venogram from the same region. Note that the spread of latencies is ± 2 s even within the motor cortex and that the latency spatially correlates with the magnitude. Also, the area where the highest signal change correlates with the longest latency and with the area where a vein is are clearly delineated in the venogram.

did not show a clear correlation of latency with evidence for draining veins (Saad and DeYoe, 1997). Fig. 12 shows functional magnitude and latency maps of the motor cortex as well as a venogram from the same region (taken from Fig. 8). Note first that the spread in latency is ± 2 s. Also note that the magnitude of the response roughly correlates with the latency, further supporting the generally observed phenomenon that large veins give the largest BOLD signal as well as the signal that is most delayed, i.e. downstream. Lastly, the venogram confirms the clear presence of larger vessels in the area of the largest latency.

Recent results (Bandettini, 1999; Menon and Kim, 1999; Menon et al., 1998) have demonstrated 'mental chronometry' involving the use of systematically varied stimuli and subsequent observation of how the hemodynamic latencies vary in correspondence to the stimuli timing. They were able to demonstrate that latency modulations on the order of 100 ms can be extracted. This type of work has also been expanded to cognitive paradigms (Richter,

Ugurbil, Georgopoulos and Kim, 1997b; Richter, Andersen, Georgopolous and Kim, 1997a).

Magnitude

The magnitude of the fMRI signal change is influenced by variables that can vary across subjects, neuronal systems, and voxels (Bandettini and Wong, 1995). To make a complete and direct correlation between neuronal activity and fMRI signal change magnitude, in a single experiment, all the variables that influence these changes must be characterized on a voxel-wise basis. Because of these primarily physiologic variables, brain activation maps will typically show a range of BOLD signal change magnitude from 1% to 5% (at 1.5 T, GE sequence, TE = 40 ms). In the past several years, considerable progress has been made in characterizing the magnitude of the fMRI signal change with underlying neuronal activity. Models have advanced considerably. Fig. 13 shows a flow chart roughly outlining both the complicating factors behind the fMRI signal as well as the richness of information contained in it.

First, as mentioned previously, it was clear that areas that showed significant BOLD signal change were in the appropriate neuronal area corresponding to specific well-characterized tasks. Second, inferred neuronal modulation was carried out by systematically varying some aspect of the task. Clear correlations between BOLD signal change magnitude and visual flicker rate, contrast, word presentation rate, and finger-tapping rate were observed (Binder et al., 1994; Kwong et al., 1992; Rao et al., 1996; Tootell, Reppas, Kwong et al., 1995). This parametric experimental design represented a significant advance in the manner in which fMRI experiments were performed, enabling more precise inferences, not about the BOLD signal change with task modulation. Still, of course, the degree of neuronal activation (i.e. integrated neuronal firing over a specified area) was still inferred.

Recently, several studies have emerged correlating measured neuronal firing rate with well known stimuli in animals (Disbrow, Slutsky, Roberts and Krubitzer, 2000) and humans (Heeger, Huk, Geisler and Albrecht, 2000; Rees, Friston and Koch, 2000), demonstrating a high correlation between BOLD signal change and electrophysiological measures. A

review article by Heeger et al. also does an excellent job in summarizing the literature linking neuronal activity (spiking rate, local field potential) with hemodynamic changes (perfusion, BOLD) (Heeger, 1999). A recent article by Logothetis, Pauls, Augath et al. (2001) using simultaneous measures of electrical activity and BOLD contrast in primate visual cortex has shown a linear relationship between neuronal activity and stimuli contrast, with one caveat: the lower the level of neuronal activity, the more BOLD contrast over-estimated the degree of neuronal activity. In other words, BOLD contrast does indeed change in proportion to the degree neuronal activity, but the relative rate at which it changes with neuronal activity is generally less. Results from this article not only impacted how fMRI signal changes are interpreted in terms of magnitude of change with a change in a task but also perhaps shed light on some issues regarding the dynamics of fMRI contrast, as described below.

Linearity

Understanding the relationship between fMRI signal change magnitude and neuronal firing rate is critically important in the better interpretation of experimental results but also in experimental design. Described above was the relationship between BOLD signal change magnitude and neuronal activity at steady state or after several seconds of continuous activity. Described in this section is the relationship between BOLD contrast and neuronal activity over time during very brief neuronal stimulation. Does BOLD signal change increase in a manner that is directly linear with stimulus duration? It has been found that, with very brief stimulus durations, the BOLD response shows a larger signal change magnitude than expected from a linear system (Boynton, Engel, Glover and Heeger, 1996; Vazquez and Noll, 1998). This greater-than-expected BOLD signal change is generally specific to stimuli durations below 3 s. Reasons for greater-than-expected event-related response may be neuronal, hemodynamic, and/or metabolic in nature. The neuronal input may not be a simple boxcar function. Instead, an increased neuronal firing rate at the onset of stimulation (neuronal 'bursting') may cause a slightly larger amount of vasodilatation than later

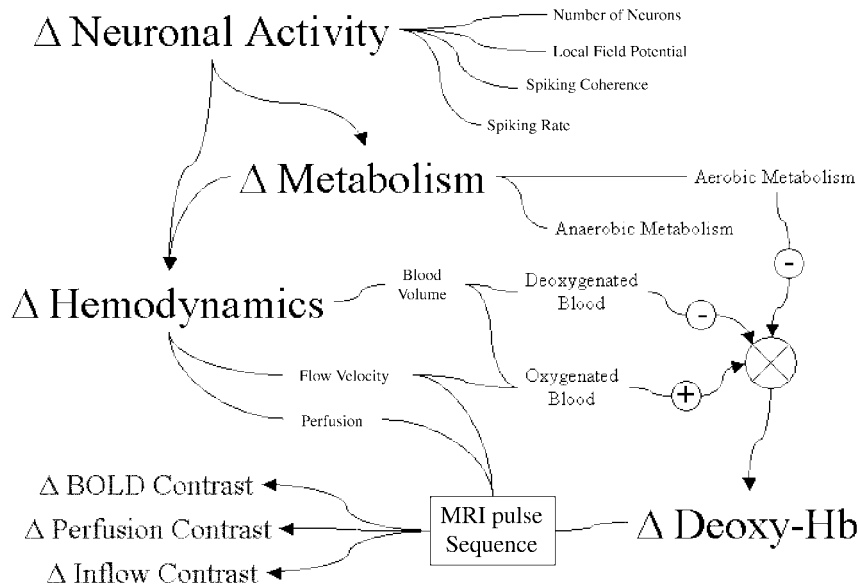


Fig. 13. Schematic diagram of the evermore complicated and interesting relationships between changes in neuronal activation, change in cerebral metabolism and hemodynamics, and changes in the appropriately weighted MRI pulse sequence.

plateaus at a lower steady state level. Results from Logothetis et al. (2001) have demonstrated clearly this ‘bursting’ at the onset of visual stimulation. In the visual cortex, this effect has been extremely well characterized in past literature describing single unit recordings.

BOLD contrast is highly sensitive to the interplay of blood flow, blood volume, and oxidative metabolic rate. If, with activation, any one of these variables changes with a different time constant, the fMRI signal may show fluctuations until a steady state is reached (Buxton, Wong and Frank, 1997; Frahm, Krüger, Merboldt and Kleinschmidt, 1996).

Recent results from Birm et al. have suggested that, based on the spatial distribution of these ‘non-linearities’ (not spatially correlated with latency or magnitude — indicators of hemodynamic characteristics) and on the fact that the transiently high signal changes remain high for about the same duration as the neuronal transients, the origin of the greater-than-expected responses may be neuronal (Bandettini and Ungerleider, 2001). A summary of these results is shown in Fig. 14. This result also gives hope in that these transient neuronal firing characteristics may be mappable, pushing fMRI signal into a new realm of interpretability.

Applications

Over the past decade, applications of fMRI have expanded as the technology, methodology, and interpretation has improved. Two primary areas of application have included basic research — understanding the organization of the healthy human brain — and clinical research.

Basic research has involved describing with greater precision and robustness, the functional anatomy of systems in the developing and adult brain that include motor, visual, auditory, tactile, taste, language, attention, emotion, learning, priming, plasticity, and memory.

Clinical research has involved two primary avenues. The first is towards robust daily clinical application. Roust clinical application depends on the creation of a means by which all types of patients can be rapidly and reproducibly scanned for the purposes of presurgical mapping, perfusion assessment, or vascular reserve assessment. Using fMRI in the clinic requires the implementation of a method by which immediate feedback is provided to the user to ensure quality control, accurate functional localization, and sufficient brain coverage, and implementation of methods by which regions of activation

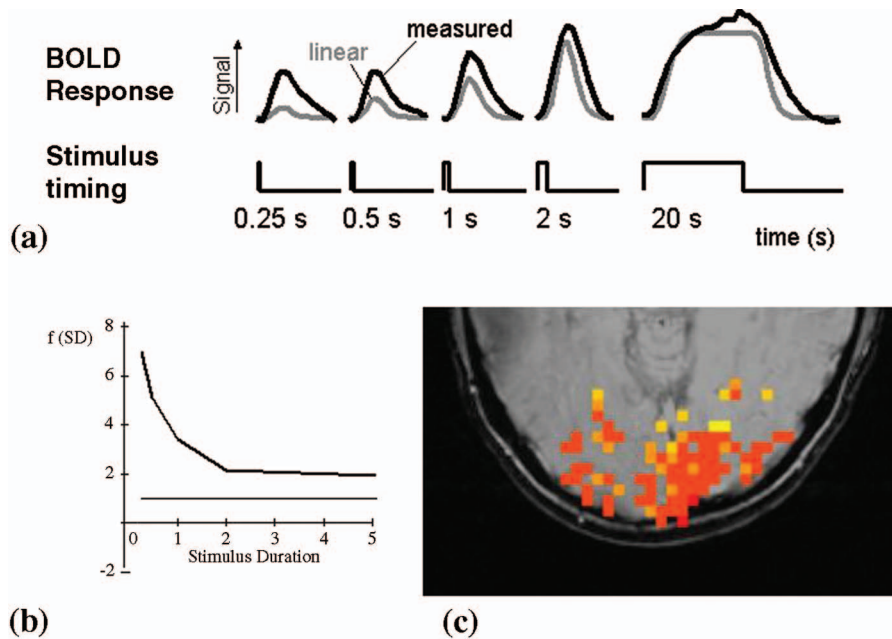


Fig. 14. (a) Summary of the dynamic nonlinearities that are commonly observed in fMRI. Short-duration stimuli elicit larger-than-expected responses. (b) The relative amplitudes of the responses vs. stimulus durations, calibrated to a long-duration stimulus duration. Note that the stimuli behave more in a more 'linear' manner after 2 s of sustained stimulation. (c) Not all voxels have the same type of nonlinear response. This is a map of the spatial heterogeneity of the dynamic nonlinearity. The two possible sources of this are neuronal or hemodynamic; an avenue of ongoing research.

are rapidly registered to useful anatomical landmarks that can then be used as guides in the context of neurosurgical procedures.

The second clinical application has been towards understanding the functional mapping correlates of specific diseases or disorders so that diagnosis may be assisted by functional imaging. Diseases that have been studied have included schizophrenia, and Alzheimer's disease. Disorders that have been studied have included obsessive-compulsive disorder, depression, dyslexia, attention deficit disorder, and addiction.

While these studies are preliminary, steady progress is being made towards using fMRI to better understand human brain organization and on a meaningful temporal and spatial scale, and to utilize this understanding towards the making of more precise diagnoses or assessments.

Conclusions

It is a truly exciting time to be using functional MRI. Issues involving methodology and interpretation are being steadily worked, technology is improving daily, and the types of questions asked in the context of the fMRI experiment are continually becoming more clever and powerful. Technology, methodology, interpretation, and applications of fMRI have been described in this chapter. The goal was that the reader would come away not only with a better perspective of what has been done and how to do it but also a sense what may be possible with fMRI in the future. Along with this perspective, it is hoped that just enough detail was supplied to give the reader insight into all aspects of fMRI and perhaps some new ideas as to how to use fMRI for their own questions. The technique has developed considerably since the first noisy signals were observed over a decade ago. More progress is certainly on the way for years to come.

References

- An H, Lin W, Celik A, Lee YZ: Quantitative measurements of cerebral metabolic rate of oxygen utilization using MRI: a volunteer study. *NMR in Biomedicine*: 14; 441–447, 2001.
- Bandettini PA: MRI studies of brain activation: dynamic characteristics. In *Functional MRI of the Brain*. Berkeley, CA: Society of Magnetic Resonance in Medicine, p. 143, 1993.
- Bandettini PA: Magnetic resonance imaging of human brain activation using endogenous susceptibility contrast. Ph.D. Dissertation. Milwaukee, WI: Medical College of Wisconsin, 1995, 1995.
- Bandettini PA: The temporal resolution of functional MRI. In Moonen CTW, Bandettini PA (Eds), *Functional MRI*. Berlin: Springer, pp. 205–220, 1999.
- Bandettini PA, Cox RW: Event-related fMRI contrast when using constant interstimulus interval: theory and experiment. *Magnetic Resonance in Medicine*: 43; 540–548, 2000.
- Bandettini PA, Jesmanowicz A, Wong EC, Hyde JS: Processing strategies for time-course data sets in functional MRI of the human brain. *Magnetic Resonance in Medicine*: 30; 161–173, 1993.
- Bandettini PA, Ungerleider LG: From neuron to BOLD: new connections. *Nature Neuroscience*: 4; 864–866, 2001.
- Bandettini PA, Wong EC: Effects of biophysical and physiologic parameters on brain activation-induced R2* and R2 changes: simulations using a deterministic diffusion model. *International Journal of Imaging Systems and Technology*: 6; 134–152, 1995.
- Bandettini PA, Wong EC, Hinks RS, Tikofsky RS, Hyde JS: Time course EPI of human brain function during task activation. *Magnetic Resonance in Medicine*: 25; 390–397, 1992.
- Belin P, Zatorre RJ, Hoge R, Evans AC, Pike B: Event-related fMRI of the auditory cortex. *Neuroimage*: 10; 417–429, 1999.
- Belliveau JW, Kennedy DN, McKinsty RC, Buchbinder BR, Weisskoff RM, Cohen MS, Vevea JM, Brady TJ, Rosen BR: Functional mapping of the human visual cortex by magnetic resonance imaging. *Science*: 254; 716–719, 1991.
- Binder JR, Rao SM, Hammeke TA, Frost JA, Bandettini PA, Hyde JS: Effects of stimulus rate on signal response during functional magnetic resonance imaging of auditory cortex. *Cognitive Brain Research*: 2; 31–38, 1994.
- Birn RM, Bandettini PA, Cox RW, Shaker R: Event-related fMRI of tasks involving brief motion. *Human Brain Mapping*: 7; 106–114, 1999.
- Birn RM, Cox RW, Bandettini PA: Detection versus estimation in event-related fMRI: choosing the optimal stimulus timing. *Neuroimage*: 15; 252–264, 2002.
- Blamire AM, Ogawa S, Ugurbil K, Rothman D, McCarthy G, Ellermann JM, Hyder F, Rattner Z, Shulman RG: Dynamic mapping of the human visual cortex by high-speed magnetic resonance imaging. *Proceedings of the National Academy of Sciences of the USA*: 89; 11069–11073, 1992.
- Boxerman JL, Bandettini PA, Kwong KK, Baker JR, Davis TL, Rosen BR, Weisskoff RM: The intravascular contribution to fMRI signal change: Monte Carlo modeling and diffusion-weighted studies in vivo. *Magnetic Resonance in Medicine*: 34; 4–10, 1995a.
- Boxerman JL, Hamberg LM, Rosen BR, Weisskoff RM: MR contrast due to intravascular magnetic susceptibility perturbations. *Magnetic Resonance in Medicine*: 34; 555–566, 1995b.
- Boynton GM, Engel SA, Glover GH, Heeger DJ: Linear systems analysis of functional magnetic resonance imaging in human V1. *Journal of Neuroscience*: 16; 4207–4221, 1996.
- Buckner RL: Event-related fMRI and the hemodynamic response. *Human Brain Mapping*: 6; 373–377, 1998.
- Buckner RL, Bandettini PA, O’Craven KM, Savoy RL, Petersen SE, Raichle ME, Rosen BR: Detection of cortical activation during averaged single trials of a cognitive task using functional magnetic resonance imaging. *Proceedings of the National Academy of Sciences of the USA*: 93; 14878–14883, 1996.
- Buckner RL, Goodman J, Burock M, Rotte M, Koutstaal W, Schacter D, Rosen B, Dale AM: Functional–anatomic correlates of object priming in humans revealed by rapid presentation event-related fMRI. *Neuron*: 20; 285–296, 1998a.
- Buckner RL, Koutstaal W, Schacter DL, Dale AM, Rotte M, Rosen BR: Functional–anatomic study of episodic retrieval. II. Selective averaging of event-related fMRI trials to test the retrieval success hypothesis. *Neuroimage*: 7; 163–175, 1998b.
- Burock MA, Buckner RL, Woldorff MG, Rosen BR, Dale AM: Randomized event-related experimental designs allow for extremely rapid presentation rates using functional MRI. *Neuroreport*: 9; 3735–3739, 1998.
- Buxton RB, Luh WM, Wong EC, Frank LR, Bandettini PA: Diffusion-weighting attenuates the BOLD signal change but not the post-stimulus undershoot. In *Proc., ISMRM 6th Annual Meeting, Sydney*, p. 7, 1998a.
- Buxton RB, Wong EC, Frank LR: A biomechanical interpretation of the BOLD signal time course: the balloon model. In *Proc., ISMRM 5th Annual Meeting, Vancouver*, 1997.
- Buxton RB, Wong EC, Frank LR: Dynamics of blood flow and oxygenation changes during brain activation: the balloon model. *Magnetic Resonance in Medicine*: 39; 855–864, 1998b.
- Cheng K, Waggoner RA, Tanaka K: Human ocular dominance columns as revealed by high-field functional magnetic resonance imaging. *Neuron*: 32; 359–374, 2001.
- Clare S, Humberstone M, Hykin J, Blumhardt LD, Bowtell R, Morris P: Detecting activations in event-related fMRI using analysis of variance. *Magnetic Resonance in Medicine*: 42; 1117–1122, 1999.
- Clark VP, Maisog JM, Haxby JV: fMRI study of face perception and memory using random stimulus sequences. *Journal of Neurophysiology*: 79; 3257–3265, 1998.
- Cohen MS: Parametric analysis of fMRI data using linear systems methods. *NeuroImage*: 6; 93–103, 1997.
- Cohen MS: Echo-planar imaging and functional MRI. In Moonen CTW, Bandettini PA (Eds), *Functional MRI*. Berlin: Springer, pp. 137–148, 1999.
- Cohen MS, Weisskoff RM: Ultra-fast imaging. *Magnetic Resonance Imaging*: 9; 1–37, 1991.
- Constable RT, Carpentier A, Pugh K, Westerveld M, Osuzan Y, Spencer DD: Investigation of the human hippocampal

?#3

- formation using a randomized event-related paradigm and Z-shimmed functional MRI. *Neuroimage*: 12(1); 55–62, 2000.
- Courtney SM, Ungerleider LG, Keil K, Haxby JV: Transient and sustained activity in a distributed neural system for human working memory. *Nature*: 386; 608–611, 1997.
- Dale A, Buckner R: Selective averaging of individual trials using fMRI. In 3rd Int. Conf. Func. Mapping of the Human Brain, Copenhagen, p. S47, 1997a.
- Dale AM: Optimal experimental design for event-related fMRI. *Human Brain Mapping*: 8; 109–114, 1999.
- Dale AM, Buckner RL: Selective averaging of rapidly presented individual trials using fMRI. *Human Brain Mapping*: 5; 329–340, 1997b.
- Davis KD, Kwan CL, Crawley AP, Mikulis DJ: Event-related fMRI of pain: entering a new era in imaging pain. *Neuroreport*: 9; 3019–3023, 1998a.
- Davis TL, Kwong KK, Weisskoff RM, Rosen BR: Calibrated functional MRI: Mapping the dynamics of oxidative metabolism. *Proceedings of the National Academy of Sciences of the USA*: 95; 1834–1839, 1998b.
- D'Esposito M, Postle BR, Ballard D, Lease J: Maintenance versus manipulation of information held in working memory: an event-related fMRI study. *Brain and Cognition*: 41; 66–86, 1999a.
- D'Esposito M, Postle BR, Jonides J, Smith EE: The neural substrate and temporal dynamics of interference effects in working memory as revealed by event-related functional MRI. *Proceedings of the National Academy of Sciences of the USA*: 96; 7514–5149, 1999b.
- D'Esposito M, Zarahn E, Aguirre GK: Event-related functional MRI: implications for cognitive psychology. *Psychological Bulletin*: 125; 155–164, 1999c.
- Detre JA, Leigh JS, Williams DS, Koretsky AP: Perfusion imaging. *Magnetic Resonance in Medicine*: 23; 37–45, 1992.
- DeYoe EA, Carman G, Bandettini P, Glickman S, Weiser J, Cox R, Miller D, Neitz J: Mapping striate and extrastriate areas in human cerebral cortex. *Proceedings of the National Academy of Sciences of the USA*: 93; 2382–2386, 1996.
- Disbrow EA, Slutsky DA, Roberts TP, Krubitzer LA: Functional MRI at 1.5 Tesla: A comparison of the blood oxygenation level-dependent signal and electrophysiology [In Process Citation]. *Proceedings of the National Academy of Sciences of the USA*: 97; 9718–9723, 2000.
- Duyn JH, Moonen CTW, van Yperen GH, Boer RWD, Luyten PR: Inflow versus deoxyhemoglobin effects in BOLD functional MRI using gradient echoes at 1.5 T. *NMR in Biomedicine*: 7; 83–88, 1994.
- Duyn JH, Tan CX, van der Veen JW, van Gelderen P, Frank JA, Ye FQ, Yongbi M: Perfusion-weighted 'single-trial' fMRI. In Proc., ISMRM 8th Annual Meeting, Denver, p. 55, 2000.
- Edelman R, Siewert B, Darby D: Qualitative mapping of cerebral blood flow and functional localization with echo planar MR imaging and signal targeting with alternating radiofrequency (EPISTAR). *Radiology*: 192; 1–8, 1994a.
- Edelman RR, Sievert B, Wielopolski P, Pearlman J, Warach S: Noninvasive mapping of cerebral perfusion by using EPISTAR MR angiography [Abstr.]. *Journal of Magnetic Resonance Imaging*: 4(P); 68, 1994b.
- Engel SA, Glover GH, Wandell BA: Retinotopic organization in human visual cortex and the spatial precision of functional MRI. *Cerebral Cortex*: 7; 181–192, 1997.
- Frahm J, Bruhn H, Merboldt K-D, Hancic W, Math D: Dynamic MR imaging of human brain oxygenation during rest and photic stimulation. *Journal of Magnetic Resonance Imaging*: 2; 501–505, 1992.
- Frahm J, Krüger G, Merboldt K-D, Kleinschmidt A: Dynamic uncoupling and recoupling of perfusion and oxidative metabolism during focal activation in man. *Magnetic Resonance in Medicine*: 35; 143–148, 1996.
- Friston KJ, Fletcher P, Josephs O, Holmes A, Rugg MD, Turner R: Event-related fMRI: characterizing differential responses. *NeuroImage*: 7; 30–40, 1998a.
- Friston KJ, Josephs O, Rees G, Turner R: Nonlinear event-related responses in fMRI. *Magnetic Resonance in Medicine*: 39; 41–52, 1998b.
- Friston KJ, Zarahn E, Josephs O, Henson RN, Dale AM: Stochastic designs in event-related fMRI. *Neuroimage*: 10; 607–619, 1999.
- Gati JS, Menon RS, Ugurbil K, Rutt BK: Experimental determination of the BOLD field strength dependence in vessels and tissue. *Magnetic Resonance in Medicine*: 38; 296–302, 1997.
- Glover GH: 3D z-shim method for reduction of susceptibility effects in BOLD fMRI. *Magnetic Resonance in Medicine*: 42; 290–299, 1999a.
- Glover GH: Deconvolution of impulse response in event-related BOLD fMRI. *Neuroimage*: 9; 416–429, 1999b.
- Glover GH, Lee AT: Motion artifacts in fMRI: comparison of 2DFT with PR and spiral scan methods. *Magnetic Resonance in Medicine*: 33; 624–635, 1995.
- Haacke EM, Lai S, Reichenbach JR, Kuppusamy K, Hoogenraad FGC, Takeichi H, Lin W: In vivo measurement of blood oxygen saturation using magnetic resonance imaging: a direct validation of the blood oxygen level-dependent concept in functional brain imaging. *Human Brain Mapping*: 5; 341–346, 1997.
- Heeger DJ: Linking visual perception with human brain activity. *Current Opinion in Neurobiology*: 9; 474–479, 1999.
- Heeger DJ, Huk AC, Geisler WS, Albrecht DG: *Nature Neuroscience*: 3; 631–633, 2000.
- Hoge RD, Atkinson J, Gill B, Crelier GR, Marrett S, Pike GB: Investigation of BOLD signal dependence on cerebral blood flow and oxygen consumption: the deoxyhemoglobin dilution model. *Magnetic Resonance in Medicine*: 42; 849–863, 1999a.
- Hoge RD, Atkinson J, Gill B, Crelier GR, Marrett S, Pike GB: Stimulus-dependent BOLD and perfusion dynamics in human V1. *Neuroimage*: 9; 573–585, 1999b.
- Jesmanowicz A, Bandettini PA, Hyde JS: Single-shot half NEX 256 × 256 resolution EPI at 3 Tesla. In Proc., ISMRM 5th Annual Meeting, Vancouver, 1997.
- Josephs O, Henson RN: Event-related functional magnetic resonance imaging: modelling, inference and optimization. *Philosophical Transactions of the Royal Society of London. Series B: Biological Sciences*: 354; 1215–1228, 1999.

- Josephs O, Turner R, Friston K: Event-related fMRI. *Human Brain Mapping*: 5; 243–248, 1997.
- Kang AM, Constable RT, Gore JC, Avrutin S: An event-related fMRI study of implicit phrase-level syntactic and semantic processing. *Neuroimage*: 10; 555–561, 1999.
- Kennan RP, Zhong J, Gore JC: Intravascular susceptibility contrast mechanisms in tissues. *Magnetic Resonance in Medicine*: 31; 9–21, 1994.
- Kiehl KA, Liddle PF, Hopfinger JB: Error processing and the rostral anterior cingulate: an event-related fMRI study. *Psychophysiology*: 37; 216–223, 2000.
- Kim S-G: Quantification of relative cerebral blood flow change by flow-sensitive alternating inversion recovery (FAIR) technique: application to functional mapping. *Magnetic Resonance in Medicine*: 34; 293–301, 1995.
- Kim S-G, Rostrup E, Larsson HB, Ogawa S, Paulson OB: Determination of relative CMRO₂ from CBF and BOLD changes: significant increase of oxygen consumption rate during visual stimulation. *Magnetic Resonance in Medicine*: 41; 1152–1161, 1999.
- Kim S-G, Ugurbil K: Comparison of blood oxygenation and cerebral blood flow effects in fMRI: estimation of relative oxygen consumption change. *Magnetic Resonance in Medicine*: 38; 59–65, 1997.
- Kwong KK, Belliveau JW, Chesler DA, Goldberg IE, Weisskoff RM, Poncelet BP, Kennedy DN, Hoppel BE, Cohen MS, Turner R, Cheng HM, Brady TJ, Rosen BR: Dynamic magnetic resonance imaging of human brain activity during primary sensory stimulation. *Proceedings of the National Academy of Sciences of the USA* 89; 5675–5679, 1992.
- Kwong KK, Chesler DA, Weisskoff RM, Donahue KM, Davis TL, Ostergaard L, Campbell TA, Rosen BR: MR perfusion studies with T1-weighted echo planar imaging. *Magnetic Resonance in Medicine*: 34; 878–887, 1995.
- Kwong KK, Chesler DA, Weisskoff RM, Rosen BR: Perfusion MR imaging. In *Proc., SMRM, 2nd Annual Meeting, San Francisco*, p. 1005, 1994.
- Lee AT, Glover GH, Meyer CH: Discrimination of large venous vessels in time-course spiral blood-oxygen-level-dependent magnetic-resonance functional neuroimaging. *Magnetic Resonance in Medicine*: 33; 745–754, 1995.
- Lee SP, Silva AC, Ugurbil K, Kim S-G: Diffusion-weighted spin-echo fMRI at 9.4 T: microvascular/tissue contribution to BOLD signal changes. *Magnetic Resonance in Medicine*: 42; 919–928, 1999.
- Liu HL, Gao JH: Perfusion-based event-related functional MRI. *Magnetic Resonance in Medicine*: 42; 1011–1013, 1999.
- Liu TT, Frank LR, Wong EC, Buxton RB: Detection power, estimation efficiency, and predictability in event-related fMRI. *Neuroimage*: 13; 759–773, 2001.
- Liu TT, Luh W-M, Wong EC, Frank LR, Buxton RB: A method for dynamic measurement of blood volume with compensation for T2 changes. In *Proc., ISMRM 8th Annual Meeting, Denver*, 2000.
- Logothetis N, Pauls J, Augath M, Trinath T, Oeltermann A: Neurophysiological investigation of the basis of the fMRI signal. *Nature*: 412; 150–157, 2001.
- McCarthy G: Event-related potentials and functional MRI: a comparison of localization in sensory, perceptual and cognitive tasks. *Electroencephalography and Clinical Neurophysiology Supplement*: 49; 3–12, 1999.
- McCarthy G, Luby M, Gore J, Goldman-Rakic P: Infrequent events transiently activate human prefrontal and parietal cortex as measured by functional MRI. *Journal of Neurophysiology*: 77; 1630–1634, 1997.
- Menon RS, Goodyear BG: Submillimeter functional localization in human striate cortex using BOLD contrast at 4 Tesla: implications for the vascular point-spread function. *Magnetic Resonance in Medicine*: 41; 230–235, 1999.
- Menon RS, Kim S-G: Spatial and temporal limits in cognitive neuroimaging with fMRI. *Trends Cogn Sci*: 3; 207–216, 1999.
- Menon RS, Luknowsky DC, Gati JS: Mental chronometry using latency-resolved functional MRI. *Proceedings of the National Academy of Sciences of the USA*: 95; 10902–10907, 1998.
- Menon RS, Ogawa S, Strupp JP, Ugurbil K: Ocular dominance in human V1 demonstrated by functional magnetic resonance imaging. *Journal of Neurophysiology*: 77; 2780–2787, 1997.
- Menon RS, Ogawa S, Tank DW, Ugurbil K: 4 Tesla gradient recalled echo characteristics of photic stimulation-induced signal changes in the human primary visual cortex. *Magnetic Resonance in Medicine*: 30; 380–386, 1993.
- Moonen CTW, vanZijl PCM, Frank JA, LeBihan D, Becker ED: Functional magnetic resonance imaging in medicine and physiology. *Science*: 250; 53–61, 1990.
- Noll DC, Cohen JD, Meyer CH, Schneider W: Spiral k-space MR imaging of cortical activation. *Journal of Magnetic Resonance Imaging*: 5; 49–56, 1995.
- Ogawa S, Lee TM: Functional brain imaging with physiologically sensitive image signals [Abstr.]. *Journal of Magnetic Resonance Imaging*: 2(P)-WIP Supplement; S22, 1992.
- Ogawa S, Lee TM, Kay AR, Tank DW: Brain magnetic resonance imaging with contrast dependent on blood oxygenation. *Proceedings of the National Academy of Sciences of the USA*: 87; 9868–9872, 1990.
- Ogawa S, Menon RS, Tank DW, Kim S-G, Merkle H, Ellerman JM, Ugurbil K: Functional brain mapping by blood oxygenation level-dependent contrast magnetic resonance imaging: a comparison of signal characteristics with a biophysical model. *Biophysical Journal*: 64; 803–812, 1993.
- Ogawa S, Tank DW, Menon R, Ellermann JM, Kim S-G, Merkle H, Ugurbil K: Intrinsic signal changes accompanying sensory stimulation: functional brain mapping with magnetic resonance imaging. *Proceedings of the National Academy of Sciences of the USA*: 89; 5951–5955, 1992.
- Patterson J, Bandettini P, Ungerleider LG: Simultaneous skin conductance measurement and fMRI during cognitive tasks: correlations of skin conductance activity with ventromedial prefrontal cortex (PFC) and orbitofrontal cortex (OFC) activity. In *Human Brain Mapping, San Antonio*, p. 235, 2000.
- Pauling L, Coryell CD: The magnetic properties and structure of hemoglobin, oxyhemoglobin, and carbon monoxyhemoglobin. *Proceedings of the National Academy of Sciences of the USA*: 22; 210–216, 1936.
- Pinel P, Le Clec HG, van de Moortele PF, Naccache L, Le Bihan

?#4

- D, Dehaene S: Event-related fMRI analysis of the cerebral circuit for number comparison. *Neuroreport*: 10; 1473–1479, 1999.
- Postle BR, D'Esposito M: 'What'-Then-'Where' in visual working memory: an event-related fMRI study. *Journal of Cognitive Neuroscience*: 11; 585–597, 1999.
- Rao SM, Bandettini PA, Binder JR, Bobholz J, Hammeke TA, Stein EA, Hyde JS: Relationship between finger movement rate and functional magnetic resonance signal change in human primary motor cortex. *Journal of Cerebral Blood Flow and Metabolism*: 16; 1250–1254, 1996.
- Rees G, Friston K, Koch C: A direct quantitative relationship between the functional properties of human and macaque V5. *Nature Neuroscience*: 3; 716–723, 2000.
- Richter W, Andersen PM, Georgopolous AP, Kim S-G: Sequential activity in human motor areas during a delayed cued finger movement task studied by time-resolved fMRI. *Neuroreport*: 8; 1257–1261, 1997a.
- Richter W, Ugurbil K, Georgopouloos A, Kim S-G: Time-resolved fMRI of mental rotation. *Neuroreport*: 8; 3697–3702, 1997b.
- Rosen BR, Belliveau JW, Aronen HJ, Kennedy D, Buchbinder BR, Fischman A, Gruber M, Glas J, Weisskoff RM, Cohen MS, Hochberg FH, Brady TJ: Susceptibility contrast imaging of cerebral blood volume: human experience. *Magnetic Resonance in Medicine*: 22; 293–299, 1991.
- Rosen BR, Belliveau JW, Chien D: Perfusion imaging by nuclear magnetic resonance. *Magnetic Resonance Quarterly*: 5; 263–281, 1989.
- Rosen BR, Buckner RL, Dale AM: Event-related functional MRI: past, present, and future. *Proceedings of the National Academy of Sciences of the USA*: 95; 773–780, 1998.
- Saad ZS, DeYoe EA: Time delay estimates of FMRI signals: efficient algorithm and estimate variance. In *Proc. 19th Annual International Conference IEEE/EMBS, Chicago*, pp. 460–463, 1997.
- Saad ZS, Ropella KM, Cox RW, DeYoe EA: Analysis and use of FMRI response delays. *Human Brain Mapping*: 13; 74–93, 2001.
- Savoy RL, Bandettini PA, Weisskoff RM, Kwong KK, Davis TL, Baker JR, Weisskoff RM, Rosen BR: Pushing the temporal resolution of fMRI: studies of very brief visual stimuli, onset variability and asynchrony, and stimulus-correlated changes in noise. In *Proc., SMR 3rd Annual Meeting, Nice*, p. 450, 1995.
- Savoy RL, O'Craven KM, Weisskoff RM, Davis TL, Baker J, Rosen B: Exploring the temporal boundaries of fMRI: measuring responses to very brief visual stimuli. In *Book of Abstracts, Society for Neuroscience, 24th Annual Meeting, Miami*, p. 1264, 1994.
- Schacter DL, Buckner RL, Koutstaal W, Dale AM, Rosen BR: Late onset of anterior prefrontal activity during true and false recognition: an event-related fMRI study. *Neuroimage*: 6; 259–269, 1997.
- Schad LR, Wiener E, Baudendistel KT, Muller E, Lorenz WJ: Event-related functional MR imaging of visual cortex stimulation at high temporal resolution using a standard 1.5 T imager. *Magnetic Resonance Imaging*: 13; 899–901, 1995.
- Sereno MI, Dale AM, Reppas JR, Kwong KK, Belliveau JW, Brady TJ, Rosen BR, Tootell RBH: Functional MRI reveals borders of multiple visual areas in humans. *Science*: 268; 889–893, 1995.
- Servos P, Zacks J, Rumelhart DE, Glover GH: Somatotopy of the human arm using fMRI. *Neuroreport*: 9; 605–609, 1998.
- Talavage TM, Ledden PJ, Sereno MI, Benson RR, Rosen BR: Preliminary fMRI evidence for tonotopicity in human auditory cortex. *Neuroimage*: 3; S355, 1996.
- Thulborn KR, Waterton JC, Matthews PM, Radda GK: Oxygenation dependence of the transverse relaxation time of water protons in whole blood at high field. *Biochimica et Biophysica Acta*: 714; 265–270, 1982.
- Tootell RB, Reppas JB, Kwong KK, Malach R, Born RT, Brady TJ, Rosen BR, Belliveau JW: Functional analysis of human MT and related visual cortical areas using magnetic resonance imaging. *Journal of Neuroscience*: 15; 3215–3230, 1995.
- Turner R, Jezzard P, Wen H, Kwong KK, Bihan DL, Zeffiro T, Balaban RS: Functional mapping of the human visual cortex at 4 and 1.5 Tesla using deoxygenation contrast EPI. *Magnetic Resonance in Medicine*: 29; 277–279, 1993.
- Turner R, LeBihan D, Moonen CTW, Despres D, Frank J: Echo-planar time course MRI of cat brain oxygenation changes. *Magnetic Resonance in Medicine*: 22; 159–166, 1991.
- vanZijl PCM, Eleff SM, Ulatowski JA, Oja JME, Ulug AM, Traystman RJ, Kauppinen RA: Quantitative assessment of blood flow, blood volume, and blood oxygenation effects in functional magnetic resonance imaging. *Nature Medicine*: 4; 159–116, 1998.
- Vazquez AL, Noll DC: Nonlinear aspects of the BOLD response in functional MRI. *Neuroimage*: 7; 108–118, 1998.
- Weisskoff RM, Boxerman JL, Zuo CS, Rosen BR: Endogenous susceptibility contrast: principles of relationship between blood oxygenation and MR signal change. In *Functional MRI of the Brain*. Berkeley, CA: Society of Magnetic Resonance in Medicine, p. 103, 1993.
- Williams DS, Detre JA, Leigh JS, Koretsky AS: Magnetic resonance imaging of perfusion using spin-inversion of arterial water. *Proceedings of the National Academy of Sciences of the USA*: 89; 212–216, 1992.
- Wong EC: Potential and pitfalls of arterial spin labelling based perfusion imaging techniques for functional MRI. In Moonen CTW, Bandettini PA (Eds), *Functional MRI*. Berlin: Springer, pp. 63–70, 1999.
- Wong EC, Bandettini PA: Simultaneous acquisition of multiple forms of fMRI contrast. In Moonen CTW, Bandettini PA (Eds), *Functional MRI*. Berlin: Springer, pp. 183–192, 1999.
- Wong EC, Bandettini PA, Hyde JS: Echo-planar imaging of the human brain using a three axis local gradient coil. In *Proc., SMRM, 11th Annual Meeting, Berlin*, p. 105, 1992.
- Wong EC, Buxton RB, Frank LR: Implementation of quantitative perfusion imaging techniques for functional brain mapping using pulsed arterial spin labeling. *NMR in Biomedicine*: 10; 237–249, 1997.
- Wong EC, Buxton RB, Frank LR: Quantitative imaging of perfusion using a single subtraction (QUIPSS and QUIPSS II). *Magnetic Resonance in Medicine*: 39; 702–708, 1998.

?#5

Wong EC, Luh W-M, T LT: Turbo ASL: arterial spin labeling with higher SNR and temporal resolution. In *Human Brain Mapping*, San Antonio, p. 452, 2000.

Yablonskiy DA: Quantitation of intrinsic magnetic susceptibility-related effects in a tissue matrix. Phantom study. *Magnetic Resonance in Medicine*: 39; 417–428, 1998.

Zarahn E, Aguirre G, D'Esposito M: A trial-based experimental design for fMRI. *NeuroImage*: 6; 122–138, 1997.

QUERIES:

- ?#1: ...to tailor the shape and (?) of the... (page 285)
- ?#2: There is no 'dashed line' in Fig. 11 as referred to in its caption. (page 287)
- ?#3: Editors' names of this volume? (page 294)
- ?#4: Journal name in full, please. (page 296)
- ?#5: Editors and Publisher? (page 297)